

DEVELOPMENT OF A RECOMBINANT NONCYTOPATHIC
BOVINE VIRAL DIARRHEA VIRUS STABLY EXPRESSING
ENHANCED GREEN FLUORESCENT PROTEIN

Except where the reference is made to the work of others, the work described in this thesis is my own or was done in collaboration with my advisory committee. This thesis does not include proprietary or classified information.

Zhenchuan Fan

Certificate of Approval:

Kenneth E. Nusbaum
Associate Professor
Pathobiology

R. Curtis Bird, Chair
Professor
Pathobiology

Sharon R. Roberts
Associate Professor
Biology

Vicky van Santen
Associate Professor
Pathobiology

Stephen L. McFarland
Dean
Graduate School

DEVELOPMENT OF A RECOMBINANT NONCYTOPATHIC
BOVINE VIRAL DIARRHEA VIRUS STABLY EXPRESSING
ENHANCED GREEN FLUORESCENT PROTEIN

Zhenchuan Fan

A Thesis

Submitted to

the Graduate Faculty of

Auburn University

in Partial Fulfillment of the

Requirements for the

Degree of

Master of Science

Auburn, Alabama

August 8, 2005

DEVELOPMENT OF A RECOMBINANT NONCYTOPATHIC
BOVINE VIRAL DIARRHEA VIRUS STABLY EXPRESSING
ENHANCED GREEN FLUORESCENT PROTEIN

Zhenchuan Fan

Permission is granted to Auburn University to make copies of this thesis at its discretion,
upon the request of individuals or institutions and at their expense. The author reserves
all publication rights.

Signature of Author

Date

Copy sent to:

Name

Date

VITA

Zhanchuan Fan, son of Mingde Fan and Xiue Guo, was born on February 11, 1974, in Sanjiao, Lin County, Shanxi Province, People's Republic of China. He attended Shanxi Agricultural University in Taigu, Shanxi, in September, 1992, and graduated with a Bachelor of Science degree in Plant Protection in June, 1996. After working in the Agricultural Bureau of Lin County, Shanxi, for one year, he entered Graduate school, China Agricultural University, Beijing, in September, 1997 and graduated with a Master of Science degree in Molecular Microbiology in July, 2000. In August, 2000, he entered Graduate School, Auburn University. He married Yanshu Li, Daughter of Zhigong Li and Biandeng Wang, on July 30, 2002.

THESIS ABSTRACT

DEVELOPMENT OF A RECOMBINANT NONCYTOPATHIC
BOVINE VIRAL DIARRHEA VIRUS STABLY EXPRESSING
ENHANCED GREEN FLUORESCENT PROTEIN

Zhenchuan Fan

Master of Science, August 8, 2005
(M.S., China Agricultural University, 2000)
(B.S., Shanxi Agricultural University, 1996)

97 typed pages

Directed by R. Curtis Bird

Noncytopathic (NCP) type-I bovine viral diarrhea virus (BVDV) strain SD1 was originally isolated from a persistently infected heifer with fatal mucosal disease (MD) and represents the only reported nucleotide sequence of a NCP BVDV isolate determined without extensive cell culture passage in the laboratory. In this study, a full length infectious cDNA clone of SD1 was constructed in a plasmid backbone, pACYC1180, a low-copy-number plasmid, by RT-PCR and standard molecular techniques. *In vitro* transcripts from this template directed the generation of infectious BVDV upon transfection of MDBK cells. The rescued virus, designated as ASD1, contained all of the artificially introduced genetic markers and had similar growth properties as wild type SD1 (wt SD1). Based on pASD1, a recombinant BVDV stably expressing enhanced

green fluorescent protein (eGFP) was successfully generated and designated as ASD1-eGFP2A3. ASD1-eGFP2A3 was stable upon passage in tissue culture and eGFP accumulated to high levels in vivo. eGFP expression was maintained stably over time following the passage of persistently-infected MDBK cells. Furthermore, ASD1-eGFP2A3 was similar to wt SD1 in viral growth properties, viral RNA replication, and viral protein expression. Thus, this marker virus may provide a tool for studying the viral transplacental infection in animal test as a real-time monitoring system and a backbone for construction of recombinant marker BVDV vaccine.

ACKNOWLEDGEMENTS

The author wishes to express his sincere gratitude to his advisor, Dr. R. Curtis Bird, for his greatest help during this studying and the members of committee, Dr. Kenneth E. Nusbaum; Dr. Sharon R. Roberts; and Dr. Vicky van Santen for their hearty support of my efforts. Special thanks go to Mrs. Allison Church Bird for her excellent technical assistance in western blotting assay.

Style manual of journal used: Virology

Computer software used: Word for Windows XP Version XP

TABLE OF CONTENTS

LIST OF TABLES	x
LIST OF FIGURES	xi
INTRODUCTION.....	1
LITERATURE REVIEW.....	3
MATERIALS AND METHODS.....	17
RESULTS.....	30
DISCUSSION.....	57
BIBLIOGRAPHY.....	60
APPENDIX.....	71

LIST OF TABLES

1. Oligonucleotides used for nucleotide sequencing.....	40
2. Oligonucleotides and template plasmids used for site-directed mutagenesis.....	41
3. Oligonucleotides used for synthesis of the subcloning adaptors.....	42
4. Oligonucleotides used for construction of subclones.....	43
5. Comparison between the viral cDNA subclones and original SD1 genome.....	44
6. Oligonucleotides used for detection of the genetic markers in ASD1.....	45

LIST OF FIGURES

1. Construction of a full length cDNA clone of BVDV SD1.....	46
2. Identification of the genetic markers in ASD1.....	47
3. Construction of cDNA clones of BVDV SD1 with the eGFP2A insert between the N ^{pro} gene and the viral capsid (C) protein gene.....	48
4. The original eGFP2A insert is not stable in the recombinant viral genome.....	49
5. The mutated eGFP2A insert is stable in the recombinant viral genome.....	50
6. eGFP2A insert does not interfere with the recombinant viral RNA replication.....	51
7. eGFP2A insert does not interfere with the recombinant viral protein expression	52
8. Comparison of viral growth kinetics between ASD1-eGFP2A3 and wt SD1.....	53
9. eGFP2A protein is expressed in ASD1-eGFP2A3-infected MDBK cells.....	54
10. eGFP2A protein is processed properly in ASD1-eGFP2A3-infected MDBK cells....	55
11. eGFP2A is maintained stably in ASD1-eGFP2A3-infected MDBK cells.....	56

INTRODUCTION

As a ubiquitous pathogen of cattle, bovine viral diarrhoea virus (BVDV) causes significant economic losses worldwide (Brownlie *et al.*, 1995). BVDV together with classical swine fever virus (CSFV) and border disease virus (BDV) was classified into the genus pestivirus of the *Flaviviridae* family which also includes two other genera of flavivirus and hepacivirus (Rice, 1996; Thiel, *et al.*, 1996). The genome of BVDV is a single-stranded, positive-sense RNA molecule of ~12.5 kb (Meyers & Thiel, 1996;) composed of a single open reading frame (ORF) flanked on both sides with a 5' untranslated region (5'-UTR) and a 3' untranslated region (3'-UTR) (Collett, *et al.*, 1991). Translation of the single ORF is cap-independently initiated at an internal ribosomal entry site (IRES) located in the 5'-UTR (Pestova, *et al.*, 1999) and the resulting viral polyprotein is processed into at least 11 mature viral proteins which are sequentially designated N^{pro}, C, E^{rns}, E1, E2, p7, NS2-3, NS4A, NS4B, NS5A, and NS5B (Elbers, *et al.*, 1996; Harada, *et al.*, 2000; Tautz, *et al.*, 1997).

Two biotype forms of BVDV, noncytopathic (NCP) and cytopathic (CP), are distinguished based on viral effects on cells in cultured tissue (Meyers & Thiel, 1996). Recently, different isolates of both forms exhibiting genetic and antigenic differences were subclassed into two genotypes: type-1 and type-2 BVDV (Pellerin, *et al.*, 1994; Becher, *et al.*, 1999; Hamers, *et al.*, 2001). Disease caused by BVDV is associated with

both acute and persistent infections. Acute infection is self-limiting and only causes subclinical or mild symptoms (Baker, 1995). However, infection of animals with NCP BVDV during the first trimester of pregnancy can result in the birth of persistently-infected calves which shed the virus for their lifetime and sporadically develop a fatal clinical syndrome, mucosal disease (MD) (Fredriksen *et al.*, 1999; Moennig & Liess, 1995). From the animals with MD, both NCP and CP BVDV strains, called a pair of biotypes, can be isolated (McClurkin, *et al.*, 1985). Considering that the pairs of biotypes are related antigenically and genetically (Pocock, *et al.*, 1987; Corapi, *et al.*, 1988), CP viruses are believed to represent the mutants developed from NCP viruses by viral genome duplication (Meyers & Theil, 1996; Tautz, *et al.*, 1996), insertion of cellular sequences (Qi, *et al.*, 1992, 1998; Mendez, *et al.*, 1998), large in-frame deletions (Tauze, *et al.*, 1994; Kupfermann, *et al.*, 1996), and even single point mutations in the NS2 region of NS2-3 (Kummerer, *et al.*, 1998, 2000). The viral genome rearrangements result in the production of discrete NS3 protein which is strictly associated with CP BVDV viruses and MD (Donis & Dubovi, 1987; Greiser-Wilke, *et al.*, 1993).

To investigate the mechanism of transplacental infection of NCP BVDV, a real-time monitoring system would help elucidate how BVDV crossed the placenta to infect the fetus. In this study, an infectious full length infectious cDNA clone of BVDV SD1, pASD1, was constructed in pACYC1180, a low-copy-number plasmid. Based on pASD1, we created an infectious marker BVD virus labeled with enhanced green fluorescent protein (eGFP). This marker virus is stable upon passage in Madin-Darby bovine kidney (MDBK) cells and the eGFP can accumulate to high levels and can be maintained stably following the passage of persistently-infected MDBK cells.

LITERATURE REVIEW

Genomic organization and viral proteins

As a single-stranded, positive-sense RNA molecule, the BVDV genome is infectious even in the absence of other viral proteins (Meyers & Thiel, 1996). Following the rapid development of molecular techniques, nucleotide sequencing of the whole BVDV genome was carried out by several different researchers. In 1985, the genomic sequence of a cytopathic (CP) BVDV strain, Osloss, was reported for the first time by Renard *et al.*, in a European Patent Application. Three years later, Collett *et al.*, (1988a) published another genomic sequence of a CP BVDV strain, NADL. In those reports, the lack of polyadenylation at the 3' end of the BVDV genome hindered the use of synthetic tandem primers to obtain cDNA clones containing genomic ends. In 1992, Brock *et al.*, developed a method to obtain tandem RNA templates using T4 RNA ligase to generate primer-directed cDNA clones. By this method, they reported the sequencing of both the 5'- and 3'-ends of CP BVDV strains NADL and 72 and noncytopathic (NCP) strain SD1 and Deng & Brock (1992) published the first complete genomic sequence of the NCP BVDV strain SD1.

With reference to the complete genomic sequence of BVDV strains Osloss, NADL, and SD1, it was found that the BVDV genome has a size ranging from 12,308 to 12,573 nucleotides (Deng & Brock, 1992). However, certain BVDV strains were

demonstrated to have considerably larger genomes of up to 16.5 kb or smaller genomes as small as up to 8 kb. At present, all of the data indicate that the larger genomes of BVDV were formed by RNA recombination through cellular RNA insertion and/or viral gene duplication (Mayer *et al.*, 1991; Qi *et al.*, 1992, 1998; Meyers & Theil, 1996; Tautz, *et al.*, 1996; Mendez, *et al.*, 1998). The smaller genomes of BVDV represent defective interfering particles formed by large in-frame deletions (Tauze, *et al.*, 1994; Kupfermann, *et al.*, 1996).

Analysis of the genomic sequences of the NADL strain and the SD1 strain revealed the genome of BVDV is composed of a single open reading frame (ORF) flanked on both sides with a 5'- untranslated region (5'-UTR) and a 3'-untranslated region (3'-UTR) (Collett, *et al.*, 1991; Poole *et al.*, 1995; Ridpath, *et al.*, 1995). The 5'-UTR of the BVDV genome harbors an internal ribosome entry site (IRES) for viral polyprotein translation and the 3'-UTR contains the signals for translation termination. Comparative analysis of BVDV genomic sequences indicated that the viral 5'-UTR contains multiple stem-loop secondary structures suggesting an important functional role of this structure and strong evolutionary pressure to avoid random mutations (Brown *et al.*, 1992; Deng & Brock, 1992). It was also reported that the BVDV genome may have substantial secondary structures which are important for viral gene expression and viral RNA replication (Collett *et al.*, 1988a; Collett *et al.*, 1989).

The BVDV genome encodes structural and nonstructural proteins for assembly of the virion and replication of viral genome, respectively. Translation of the unique viral ORF is cap-independently initiated at the IRES (Poole, *et al.*, 1995; Pestova, *et al.*, 1999) and results in a polyprotein of about 4000 amino acids which is cleaved into the mature

viral proteins by host-cell or virus-encoded proteases with a co-translational and/or a post-translational processing strategy (Elbers, *et al.*, 1996; Harada, *et al.*, 2000; Tautz, *et al.*, 1997). For NCP BVDV strains, 11 mature viral proteins are detected as follows: COOH-N^{pro}, C, E^{ms}, E1, E2, P7, NS2-3, NS4A, NS4B, NS5A, and NS5B-NH₂. However, for CP BVDV strains, in addition to these viral proteins, separate viral proteins of NS2 and NS3 are invariably expressed.

The protein processed from the N-terminus of viral polyprotein is a nonstructural protein N^{pro} (N^{pro}, amino-terminal protease) which cleaves itself from the viral polyprotein as a cysteine protease (Wiskerchen, *et al.*, 1991; Stark, *et al.*, 1993; Rumenapf, *et al.*, 1998). N^{pro} is unique to pestiviruses and there is no homologous viral protein detected in the flaviviruses and haptavirus. Recently, it was found that N^{pro} is not just a serine protease but, at least partially, responsible for viral interference in cellular antiviral defenses (Horscroft, *et al.*, 2005). A small 14 kD viral protein, C, immediately downstream from N^{pro}, was found to be well conserved among pestiviruses (Sullivan *et al.*, 1994; Donis, 1995) and has been speculated to be the viral capsid protein of BVDV (Thiel *et al.*, 1991; Sullivan *et al.*, 1994). Immediately following C are 3 viral structural glycoproteins: E^{ms} (gp48), E1 (gp25), and E2 (gp53). E^{ms} forms a disulfide-bonded homodimer (Rumenapf *et al.*, 1993; Konig *et al.*, 1995) and has an intrinsic RNase activity (Hulst, *et al.*, 1994; Schneider *et al.*, 1993; Windisch *et al.*, 1996). Recently, the C-terminal domain of E^{ms} was shown to have the ability to translocate across eukaryotic cell membranes (Langedijk, 2002). Additionally, both E^{ms}-E2 and E2-E1 heterodimers are present in viral envelope (Lazar, *et al.*, 2003) and E2-E1 heterodimer was thought to be the major complex of mature virion (Weiland *et al.*, 1990; Branza-Nichita *et al.*, 2001).

E2 protein appears to be involved in the attachment and/or penetration of the viral sequences into host cells (Xue & Minocha, 1993) and was characterized as an immunodominant protein to which neutralizing monoclonal antibodies (Mabs) were directed (Donis *et al.*, 1988; Collett, 1992).

Immediately following E2 in the viral polyprotein are the viral nonstructural proteins including P7, NS2-3, NS4A, NS4B, NS5A, and NS5B. Among them, it was reported that P7 is indispensable for the assembly of infectious virion (Harada *et al.*, 2000). Release of the viral proteins located downstream of NS2-3 is mediated by a serine protease within the NS3 region of NS2-3 together with NS4A as a cofactor (Tautz *et al.*, 1997; Wiskerchen, *et al.*, 1991; Xu, *et al.*, 1997). The NS3 region also has helicase and NTPase activities that are dispensable for viral replication (Grassmann, *et al.*, 1999; Gu, *et al.*, 2000). NS5B was identified as the viral RNA-dependent RNA polymerase (RdRp) which is responsible for viral RNA replication (Collett, 1992; Kao, *et al.*, 1999; Lohman, *et al.*, 1999; Zhong, *et al.*, 1998).

Biotypes and genotypes

In 1957, Lee and Gillespie first reported an isolate of BVDV which did not induce detectable cytopathology in cell culture and, in the same year, Underdahl *et al* (1957) reported an isolate of BVDV which induced cytopathology in tissue culture. Based on the differential viral ability to generate cytopathic effect in cultured cells, BVDV was classified into two biotypes: noncytopathic (NCP) and cytopathic (CP) (Meyers & Thiel, 1996). It has been shown that both biotypes of BVDV could be isolated from cattle with mucosal disease (MD) and such pairs of biotypes had similar viral growth characteristics (Howard *et al.*, 1987; Corapi *et al.*, 1988) and were related antigenically (Taylor *et al.*,

1963; Castrucci *et al.*, 1975) and genetically (Donis and Dubovi, 1987b; Meyers *et al.*, 1992; Tautz *et al.*, 1994). Therefore, it was hypothesized that the CP BVDV strains isolated from cattle with MD arose by mutation of the pre-existing persistent NCP BVDV strains (Brownlie *et al.*, 1987., Corapi *et al.*, 1988). Nucleotide sequence analysis of CP and NCP paired isolates derived from single MD cases indicated that the virus pairs are very closely related, which added support for a mutational hypothesis (Meyers *et al.*, 1991; Meyers *et al.*, 1992).

It has been demonstrated that a separate 80 kD viral protein, NS3, is strictly associated with CP viruses, however, only NS2-3 viral protein could be found in cells infected with NCP viruses (Donis and Dubovi, 1987b; Pocock *et al.*, 1987). Thus, it was speculated that the expression of NS3 determines the cytopathogenicity of BVDV isolates (Tautz *et al.*, 1994). Over past years, evidence has shown that separated NS3 generation was due to an insertion of cellular sequences into the viral genome (Qi *et al.*, 1992; De Moerlooze *et al.*, 1993; Mendez, *et al.*, 1998), duplication of the virus genomes (Meyers *et al.*, 1992; Meyers & Theil, 1996; Tautz, *et al.*, 1996), deletion within the virus genome (Tautz *et al.*, 1994; Kupfermann, *et al.*, 1996), or even point mutations in the NS2 region of NS2-3 (Kummerer, *et al.*, 1998, 2000). So it was believed that RNA recombination caused by template switching leads to the production of NS3 (Meyers *et al.*, 1991; Qi *et al.*, 1992; Meyers *et al.*, 1992).

At present, it is known that only the NCP biotypes can induce persistent infections although both biotypes are capable of crossing the placenta to infect the fetus (Bolin *et al.*, 1988). Studies have demonstrated that infection of pregnant cows with NCP BVDV strains resulted in the birth of calves that were persistently infected (PI) and were

immunotolerant with respect to the particular BVDV strain following *in utero* infection (Bolin *et al.*, 1988). The immunotolerance has been demonstrated to be a strain-specific immune response against antigenically different BVDV strains and is incapable of eliminating persistent BVDV (Coria and McClurkin, 1978; Bolin *et al.*, 1988; Moenning *et al.*, 1990). There have been no reports of experimental production of PI animals with CP strains as well as no case reports in which CP viruses were isolated from a persistently infected animal in the absence of a NCP virus (McClurkin *et al.*, 1984; Brownlie *et al.*, 1989). The vast majority of clinical isolates of BVDV have been NCP strains which have maintained themselves in the bovine population through the production of persistently infected cattle (Moenning and Plagemann, 1992).

Ridpath *et al.*, (1994) identified two distinct genetic lineages of BVDV by comparing the nucleotide sequences of the 5'-UTR and the genomic region coding for the NS2-3 protein of 140 BVDV isolates. Recently, two genotypes of BVDV, BVDV type I (BVDV-I) and BVDV type II (BVDV-II) have been designated based on 5'-UTR nucleotide sequences and E2 Mab analysis (Xue *et al.*, 1990; Pellerin, *et al.*, 1994; Becher, *et al.*, 1999; Hamers, *et al.*, 2001). The 5'-UTR is highly conserved in BVDV genome compared to the rest of the viral genome, so differences in the 5'-UTR tend to be significant rather than due to random variation although differences between type-I and type-II BVDV strains exist throughout the whole viral genome. Also, differences in acute pathogenesis also exist between the genotypes. It was reported that severe acute (SA) disease, which was proven to be lethal to cattle, has only been reported with type-II BVDV strains. However, it should be noted that type-2 strains causing SA are in the minority and most type-II BVDV strains are no more virulent than type-I BVDV strains.

NCP BVDV strain SD1 and laboratory strains of BVDV such as CP NADL and Osloss were suggested to belong to type-I BVDV lineages. Comparison of the nucleotide sequences among these classical strains revealed a sequence homology of nearly 78% to 88% for the entire genome. Conserved regions such as the 5'-UTR of these viruses had homologies ranging from 86% to 93% among these strains. It was demonstrated that type-II BVDV isolates which caused severe outbreaks were only 75% homologous to the type-I strains within the 5'-UTR region, but were more than 90% homologous in the 5'-UTR as a group. (Ridpath *et al.*, 1994).

Immune responses and antigenic diversity

BVDV induces both humoral and cellular immune responses (Hulst *et al.*, 1993). Live BVDV induces production of antibodies against E^{tns}, E1, E2, and NS3/NS2-3 viral proteins (Bolin and Ridpath, 1989). However, killed BVDV only stimulates generation of antibodies against E^{tns}, E1 and E2 proteins (Bolin and Ridpath, 1990). NS3/NS2-3 and E2 were shown to be immunodominant (Bolin and Ridpath, 1989, 1990; Collett, 1992). Three to four antigenetic domains are presented within the viral E2 protein, the major antigenetic epitope (Ridpath *et al.*, 1994; Xue *et al.*, 1990), and the appropriate conformation of the E2 epitope may be necessary for an effective antibody response (Kamstrap *et al.*, 1991; Paton *et al.*, 1992). The serologic cross-reactivity between BVDV genotypes I and II has been reported to be relatively low, which may indicate a distinct genotypic antigenic site located on the E2 proteins of genotype I and II BVDV (Pellerin *et al.*, 1994; Ridpath *et al.*, 1994). It was reported that CD4⁺ cells play a pivotal role in the establishment of immune memory to BVDV (Howard *et al.*, 1992). However, the major T-cell antigens have not been determined (Bolin, 1993; Kimman *et al.*, 1993).

It was indicated that the level of the immune response in PI cattle may be attenuated considerably (Roberts *et al.*, 1988). However, the PI cattle are immunocompetent to various antigens including those expressed by a heterologous BVDV strain (Moennig *et al.*, 1990). It has also been shown that both neutralizing and non-neutralizing antibodies to the persistent virus were absent in PI cattle (Donis and Dubovi, 1987b) and that persistence of BVDV in cattle was associated with specific T-cell immunotolerance (Coria and McClurkin, 1978). BVDV has affinity for replication in lymphocytes (Lopez *et al.*, 1993) and this may play a role in the establishment of tolerance and perhaps interferes with lymphocyte function. Considerable evidence has accumulated that BVDV infection results in immunosuppression of the host (Howard, 1990; Atluru *et al.*, 1992). Following infection, BVDV antigen has been detected in most of the hematopoietic cells including lymphocytes, macrophages and neutrophils (Jensen *et al.*, 1991; Atluru *et al.*, 1992; Lopez *et al.*, 1993).

In vitro studies demonstrated that BVDV suppresses the proliferative response and interleukin-2 production of lymphocytes from normal calves induced by a T lymphocyte specific mitogen, phytohemagglutinin (Atluru *et al.*, 1990). Recently, it was reported that CP BVDV strains induce the synthesis of interferon α/β in infected macrophages (Perler, *et al.*, 2000; Schweizer, *et al.*, 2001) and killed their host by apoptosis (Zhang, *et al.*, 1997; Schweizer, *et al.*, 1999). However, NCP BVDV strains are resistant to the potent pro-apoptotic and interferon (IFN)-inducing effects of dsRNA *in vitro* (Schweizer, *et al.*, 2001).

Virus neutralization tests and cross-protection studies established that distinct serotypes of BVDV did not exist and that protection from clinical disease could be

obtained by prior exposure to any isolate of BVDV (Baker, 1987). However, evidence for antigenic diversity among strains of BVDV was established through the use of cross-neutralization studies with the development of BVDV-E2-specific monoclonal antibodies (Mabs) in the late 1980s (Xue *et al.*, 1990). Other studies have focused on the antigenicity of the immunodominant nonstructural protein NS3 (p80). Several conserved epitopes have been identified on the NS3 protein among the pestiviruses (Paton *et al.*, 1991)

Mabs have been extremely helpful and have been used successfully to distinguish CSFV from BVDV and BDV (Cay *et al.*, 1989) and to detect all strains of CSFV (Wensvoort *et al.*, 1989). However, Mabs have not provided the ability to separate BVDV isolates into distinct groups (Dubovi, 1992). Although there apparently had been reports of BVDV-specific Mabs, studies that attempted to subdivide BVDV strains into antigenic groups failed to provide confirmation of the ability to definitively discriminate meaningful strain differences (Corapi *et al.*, 1988; Xue *et al.*, 1990; Deregt *et al.*, 1994).

Viral pathogenesis and laboratory diagnostics

BVDV can cause acute infections with a wide spectrum of subclinical symptoms or persistent infections which sporadically lead to the production of animals with MD, a highly fatal disease (Baker, 1990; Bolin, 1993). It was reported that both NCP and CP biotypes can induce acute infections; however, only NCP biotype can induce persistent infections (Baker, 1990; Bolin, 1993).

It has been reported that NCP BVDV can result in embryonic death, resorption, stillbirth, or even induce birth of the PI calves when the fetuses were infected *in utero* by NCP BVDV strains, between approximately 30 days and 120 days of gestation, prior to

the full development of their immune systems (Radostits and Littlejohns, 1988; Baker, 1990; Kirkland *et al.*, 1993). PI cattle can sporadically develop MD if super-infection with an antigenically similar CP virus occurs (Baker, 1990; Moening *et al.*, 1990). MD, a rare, fatal disease, was reported to have occurred in PI cattle ranging in age from 6 months to 2 years with a low morbidity generally (David *et al.*, 1994; Taylor *et al.*, 1994). PI cattle often appeared and served as natural reservoirs for BVDV by continually shedding virus in their secretions and excretions (Baker, 1987). Studies demonstrated that both NCP and CP BVDV strains with similar antigenicity could be isolated from one animal with MD and such viruses have been called a virus pair (Bromnillie, 1990). In addition, it was also reported that antigenically distinct NCP and CP pairs of BVDV strains can induce MD (Ridpath *et al.*, 1991). Recent studies revealed that different CP BVDV strains evolved from NCP strains most likely by a process of RNA recombination, e.g. the uptake of cellular inserts (Meyers *et al.*, 1991, 1992; Qi, *et al.*, 1992; De Moerlooze *et al.*, 1993; Mendez, *et al.*, 1998), duplication of the virus genomes (Meyers *et al.*, 1992; Meyers & Theil, 1996; Tautz, *et al.*, 1996), or deletion within the virus genome (Tautz *et al.*, 1994; Kupfermann, *et al.*, 1996). However, as inserts or deletions have not been identified in all CP BVDV examined, it appears that recombination may not be the only mechanism involved in biotype determination (Kummerer, *et al.*, 1998, 2000).

BVDV-1 strains and majority of BVDV-2 strains induce mild acute infections characterized by fever and diarrhea in which the majority of animals recover (Baker, 1990). However, some NCP BVDV-2 can induce severe acute (SA) infections characterized by fever, diarrhea, lymphopenia, thrombocytopenia, hemorrhage and even

death (Corapi *et al.*, 1989, 1990; Bolin and Ridpath, 1992; Hibberd *et al.*, 1993; Carman *et al.*, 1994; David *et al.*, 1994).

Different methods have been developed for detection of BVDV including immunofluorescence assays (IFA) and immunoperoxidase staining (IPS), virus isolation (VI), virus neutralization (VN), enzyme-linked immunosorbent assays (ELISA), and reverse transcriptase PCR (RT-PCR) (Boye *et al.*, 1991; Brock, 1991; Ridpath and Bolin, 1991; Hooft van Iddekinge *et al.*, 1992; Alansarki *et al.*, 1993, Ridpath *et al.*, 1993).

Virus isolation is the most reliable and widely used method for the diagnosis of BVDV infection. BVDV can be isolated from whole blood or tissues of viremic animals on susceptible cell cultures (Dubovi, 1990). The CP isolates can be identified in cell culture directly and the NCP isolates can be consistently identified by indirect methods (Dubovi, 1990). BVDV has a marked tropism for lymphoid tissue/cells (Baker, 1987). Thus, the tissues from these organs are the best biopsy locations for viral antigen detection using immunohistochemical methods such as IFA or IPS (Dubovi, 1990). Mabs specific for BVDV, such as 15C5 and D89, allow reliable and easy identification of BVDV and discrimination from other pestiviruses (Haines *et al.*, 1992).

VN is relatively simple to perform and interpret; however, the obvious shortcoming is that paired serum samples are needed to make a definitive diagnosis and there has been no standard reference strain of BVDV. Therefore, in most of the cases, CP strains of BVDV have been used in order to easily detect the neutralization of the viruses. NCP strains may be used as reference strains in tests with virus neutralization end points detected by Mabs conjugated to peroxidase (Dubovi, 1990; Afshar *et al.*, 1991). Due to the antigenic differences that exist among BVDV isolates, the reported antibody titer for

a specific serum sample may vary greatly from laboratory to laboratory, depending on the reference strain of BVDV used in the virus neutralization test (Bolin *et al.*, 1991).

Several different antigen capture ELISAs have been developed using BVDV specific Mabs (Fenton *et al.*, 1990; Shannon *et al.*, 1991; Gottschalk *et al.*, 1992). Detection is usually achieved using polyclonal antibodies conjugated with peroxidase. These types of ELISAs are reliable and have been shown to correlate well with the more protracted and labor-intensive technique of virus isolation.

With the availability of the nucleotide sequence of BVDV, detection of viral RNA by RT-PCR has become an important method for detection of BVDV in laboratory diagnosis due to the increase in precision, specificity, and speed of completion compared to the ELISA assays. At present, RT-PCR has been reported by several researchers (Boye *et al.*, 1991; Brock 1991; Ward and Misra, 1991; Alansarki *et al.*, 1993; Katz *et al.*, 1993; Ridpath *et al.*, 1993). In this kind of test, the choice of primers was critical and was based on conserved motifs, such as the nonstructural NS2-3 region and the 5'-UTR, within the genome so that widely divergent virus were not missed (Gruber *et al.*, 1993; Ridpath *et al.*, 1993; Desport *et al.*, 1994).

Prevention and control

At present, two measures have been used to prevent and control the infection of BVDV: identification and removal of the persistently-infected animals and vaccination of animals to increase immunity to the disease (Ames and Baker, 1990; Hjerpe, 1990). Currently, two types of BVDV vaccines are used: inactivated and modified-live virus vaccines. In general, inactivated vaccines, although safer, do not provide broad fetal protection and only provide short-lived humoral immunity lasting 3 to 6 months

(Hjerpe, 1990; Harkness *et al.*, 1986; Meyling *et al.*, 1987; Bolin *et al.*, 1991). Modified-live vaccines contain CP strains of BVDV that have been attenuated by continuous cell culture passage (Hjerpe, 1990) and are not approved for use in pregnant animals due to the risk of causing abortion and congenital defects ((Liess *et al.*, 1984). Also, the reverse mutation of the modified-live vaccines is another concern indeed.

Considering that all BVDV are antigenically related (Bolin and Ridpath, 1992), vaccination with a single strain of BVDV should offer some protection to other BVDV strains (Bolin and Ridpath, 1990). However, with an increasing awareness of antigenic diversity of BVDV, vaccination programs have been recommended to attempt to induce high serologic antibody concentration against a broad range of BVDV strains including both BVDV I and BVDV II (Bolin *et al.*, 1991; Dubovi, 1992; Pellerin, *et al.*, 1994; Bolin *et al.*, 1991; Cortese, 1994) based on the rationale that the serologic cross-reactivity between BVDV I and II was relatively low (Pellerin *et al.*, 1994; Ridpath *et al.*, 1994) and cross protection between BVDV I and BVDV II was not sufficiently efficient to prevent transplacental infection (Ridpath *et al.* 1994). The progress to achieve this aim is really slow and there are no published articles for reference.

To decrease exposure of cattle to the BVDV pathogen, practices aimed at preventing introduction of BVDV to farms have been suggested for breeding operations, including dairy and beef cattle operations, but these have proven impractical for feedlot or veal operations (Ames and Baker, 1990). In addition, wild ruminants, such as deer, may serve as an outside, and much more difficult to control, reservoir for BVDV (Nettleton, 1990). PI animals have been sources of virus for other animals and especially their offspring (Bezek and Mechor, 1992). Thus, detection and elimination of PI animals from herds

with a history of BVDV associated disease has been recommended as of the utmost importance in resolving the disease problem in the hope that a combination of vaccination plus breeding operation management can control the spread of BVDV (Ames and Baker, 1990; Bezek and Mechor, 1992).

To prevent BVDV infection of cattle during gestation by vaccination, a question should be answered first: how does BVDV cross the placenta to infect the fetus? One promising approach to elucidating this mechanism would be to construct a live-marked BVD virus so that the spread of the virus *in vivo* could be monitored by a real-time method. To avoid impairing the pathogenic ability of the BVDV pathogen, we chose to insert a fluorescent GFP protein between the viral N^{pro} protein and capsid (C) protein and determine if pathogenesis of recombinant fluorescent BVDV was comparable to the wt SD1 strain of BVDV.

MATERIALS AND METHODS

Cell, viruses, bacterial strains, and antisera

Madin-Darby bovine kidney (MDBK) cells were kindly provided by Kenny V. Brock, DVM, Ph.D. (Department of Pathobiology, Auburn University) and incubated in Dulbecco's modified Eagles medium (DMEM) (Fisher Scientific, Pittsburgh, PA) supplemented with 10% horse serum, 10% L-glutamine, 10 U/ml of penicillin, and 10 µg/ml of streptomycin. The noncytopathic type-1 BVDV strain SD1 was kindly provided by Dr. Kenny V. Brock and described previously (Deng & Brock, 1992). Recombinant viruses, ASD1, ASD1-eGFP2A1, ASD1-eGFP2A2, and ASD1-eGFP2A3, were generated as part of this study. *Escherichia coli* XL1-Blue was purchased from Stratagene (La Jolla, CA). Polyclonal antisera B224, specific against BVDV, was provided by Dr. Kenny V. Brock.

Oligonucleotides and plasmid vectors

Oligonucleotides for sequencing (TABLE 1), site-directed mutagenesis (TABLE 2) and cloning adaptors (TABLE 3) were designed based on the published nucleotide sequence of the SD1 genome (Genbank Accession No. M96751). All oligonucleotides were purchased from Sigma Genosys (Woodlands, TX). pUC19 and pACYC1180 were purchased from New England Biolabs (Beverly, MA). pBAD24 was kindly provided by Dr. Haihong Wang (Microbiology lab, College of Life Science, South China Agricultural

University). Subcloning vector pUCMCS was derived by inserting the cloning adaptor, PUCMCS (generated by annealing PUCPOSF and PUCNEGF), between the *NarI* and *HindIII* sites of pUC19. pUCNDEH was derived by inserting the cloning adaptor, PUCNEH (created by annealing PUCNEHP and PUCNEHN), between the *EcoRI* and *HindIII* sites of pUC19 in which the *NdeI* site at position 183 was inactivated by site-directed mutagenesis. pBADEH was obtained by inserting the cloning adaptor of PUCNEH between the *EcoRI* and *HindIII* sites of pBAD24. peGFP was purchased from Clontech (Palo Alto, CA)

Site-directed mutagenesis

Site-directed mutagenesis was performed with a Quickchange site-directed mutagenesis kit (Stratagene) as described by manufacturer. A pair of complementary primers for mutagenesis and 50 ng of plasmid template were used in a 50 μ l system. PCR was performed with cloned *Pfu* polymerase (Stratagene) for 12 cycles for point mutations and for 16 cycles for multiple nucleotide insertions or deletions. The working parameters were as following: 95°C for 1 min to denature the template plasmid DNA, 48°C to 70°C for 45 sec to allow primer annealing and 70°C for 3-14 min for DNA extension. The methylated template plasmid DNA was removed from the PCR products by digestion with *DpnI* (Stratagene) at 37°C for 1 hr. Then, the PCR products were transformed into *Escherichia coli* XL1-Blue and the presence of desired mutations and insertions were verified by nucleotide sequencing.

Nucleotide sequencing

Nucleotide sequencing was performed at Auburn University Genomics & Sequencing laboratory. Nucleotides were read on an ABI3100 Genetic Analyzer (Applied

biosystems, Foster City, CA) and the sequence analyzed with the DNAMAN program (Lynnon Corporation, Quebec, Canada).

Construction of viral cDNA clones spanning the whole genome of SD1

MDBK cells were infected with wt SD1 at a multiplicity of infection (MOI) of 1.0 FFU/cell. After 72 hr incubation at 37°C, viruses were harvested from the supernatant and viral RNA was extracted from 300 µl supernatant using a QIAamp Viral RNA mini kit (Qiagen, Valencia, CA) as described by the manufacturer. The viral RNA obtained was suspended in 100 µl nuclease-free water and stored at -80°C until use. RT-PCR was performed employing a two-step method. The RT step was done with M-MLV reverse transcriptase (Promega) in a 25 µl system (13 µl viral RNA, 1 µl 20 ng/µl anti-sense primer, 5 µl 5×reaction buffer, 5 µl dNTP solution, and 1 µl M-MLV reverse transcriptase). After 13 µl viral RNA and 1 µl anti-sense primer were mixed in 0.2 ml thin wall tube, the tube was heated to 70°C for 5 min to melt secondary structure within the viral RNA templates and then cooled immediately on ice to prevent viral RNA secondary structure from reforming. The first-strand cDNA synthesis was performed at 42°C for 1 hr after addition of 5 µl 5×reaction buffer, 5 µl dNTP solution, and 1 µl M-MLV reverse transcriptase to the tube. PCR amplification was performed in a 50 µl system using PCR Master Mix (Promega) with the following reaction parameters: 95°C for 2 min followed by 40 cycles of 95°C for 1 min, 53°C for 45 sec, and 72°C for 90 sec. By RT-PCR amplification, seven cDNA fragments overlapping the genome of BVDV SD1 were synthesized from viral RNA using oligonucleotides as shown in Table 4. All seven cDNA fragments were individually purified with a Qiaquick PCR purification kit (Qiagen), double digested with the selected restriction enzymes, and subcloned into the

vectors, pUCMXS or pUCNDEH. Data from nucleotide sequencing showed that there were a total of 12 mutations present in these subclones (TABLE 5) compared to the published nucleotide sequence of SD1. Using site-directed mutagenesis, the coding mutations and deletions were repaired and the noncoding mutations including T7585C, G7882C, G9022A, A10912G, and A12264G were employed as genetic markers. Thus, the final subclones composing the entire BVDV genome included pSDXN1 (1-1,916, *XbaI-NdeI* fragment), pSDNF (1,917-4,209, *NdeI-FseI* fragment), pSDFN1 (4,209-6,037, *FseI-NsiI* fragment), pSDNE2 (6,037-6,900, *NsiI-EagI* fragment), pSDEN (6,901-8,461, *EagI-NcoI* fragment), pSDNN1(8,462-10,126, *NcoI-NdeI* fragment), and pSDNP2 (10,127-12,319, *NdeI-PacI* fragment).

Plasmid constructs

PCR was performed with *Pfu* DNA polymerase (Stratagene, La Jolla, CA). Plasmids were constructed by standard techniques and confirmed by nucleotide (nt) sequencing (Sambrook, *et al.*, 1989). The oligonucleotides were designed based on the published sequence of the SD1 genome (Deng & Brock, 1992; Genbank Accession No. M96751) and purchased from Sigma Genosys. The restriction enzymes were purchased from New England Biolabs. The oligonucleotides for subcloning are listed (Table 4).

pASD1 A 1.9 kb *XbaI-NdeI* fragment isolated from pSDXN1 and a 2.3 kb *NdeI-PacI* fragment isolated from pSDNF were subcloned into the *XbaI-PacI* sites of the pACNR1180 vector by three-way ligation resulting in pACXF harboring the 5' half of the SD1 genome (nt 1 to 4,203) preceded by a T7 promoter. By standard recombinant techniques, a 1.8 kb *FseI-NsiI* fragment of pSDFN1, a 0.9 kb *NsiI-EagI* fragment of pSDNE2, a 1.5 kb *EagI-NcoI* fragment of pSDEN, a 1.7 kb *NcoI-NdeI* fragment of

pSDNN1, and a 2.4 kb *NdeI-PacI* fragment of pSDNP2 were subcloned into the pBADEH vector step by step resulting in pBADFP containing the 3' half of the SD1 genome (nt 4,204 to 12,319) followed by an engineered *SdaI* site. Finally, an 8.1 kb *FseI-PacI* fragment was isolated from pBADFP and subcloned into the *FseI-PacI* sites of pACXF resulting in a full-length cDNA clone of SD1, pASD1.

peGFP2A1 A 51 bp *BsrGI-NotI* fragment, encoding foot-and-mouth disease virus 2A protease (FMDV 2A^{pro}), was obtained by annealing two oligonucleotides of PGFP2AP (5'-CCTTGGATTTTAATCATGAATAGAA-3') and PGFP2AN (5'-TTCTATTCATGATTAAAATCCAAGG-3') and extending them with Klenow fragment (Promega, Madison, MI) as described by the manufacturer. This fragment was subcloned into the *BsrGI-NotI* sites of the peGFP vector (Clontech) resulting in peGFP2A1 in which the FMDV 2A^{pro} fragment was inserted in frame immediately downstream of eGFP gene.

pASD1-eGFP2A1 A 1 kb *XbaI-KpnI* fragment, corresponding to nt 1 to 917 of the SD1 genome, was amplified from pSDXN1 using oligonucleotides SD1-T7-*XbaI* (5'-CCCGAGGTGATGGAAGGGGAAGATC-3') and SD1-917-*KpnI* (5'-GTTGGTACCTCTTTTGTACTGAGCAGC-3'). A 1 kb *ApaI-NdeI* fragment, corresponding to nt 890 to 1924 of the SD1 genome, was amplified from pSDXN1 using oligonucleotides SD1-890-*ApaI* (5'-GTCGGGCCCTCAGATACAAAAGAAGAAGG-3') and SD1-1924-*NdeI* (5'-AAACCATATGTAGCCAATTTTTCGATCGAC-3') and was subcloned into the *ApaI-NdeI* sites of the pSDXN1 vector resulting in pFAN8. An 800 bp *KpnI-ApaI* eGFP2A fragment was amplified from peGFP2A1 using oligonucleotides eGFP2A-up-*KpnI* (5'-CATGGGCCCATGGTGAGCAAGGGCGAGG-3') and eGFP2A-down-*KpnI* (5'-CATGGTACCATGGGCCCTGGGTTGGACTCG-3'). Then, the 1 kb

XbaI-KpnI fragment and the 800 bp *KpnI-ApaI* eGFP2A fragment were subcloned into the *XbaI-ApaI* sites of the pFAN8 vector by three-way ligation resulting in pFAN12. A 2.7 kb *XbaI-NdeI* fragment was isolated from pFAN12 and subcloned into the *XbaI-NdeI* sites of the pACXF vector resulting in pACXF-eGFP2A-16. Finally, an 8.1 kb *FseI-PacI* fragment was isolated from pBADFP and subcloned into the *FseI-PacI* sites of the pACXF-eGFP2A-16 vector resulting in pASD1-eGFP2A1.

pASD1-eGFP2A2 A 1 kb *ApaI-NdeI* fragment, corresponding to nt 893 to 1924 of the SD1 genome, was amplified from pSDXN1 using oligonucleotides SD1-893-*ApaI* (5'-GTCGGGCCCGATACAAAAGAAGAAGGAGC-3') and SD1-1924-*NdeI* and subcloned into the *ApaI-NdeI* sites of the pSDXN1 vector resulting in pFAN9. Then, the 1 kb *XbaI-KpnI* fragment and the 800 bp *KpnI-ApaI* eGFP2A fragment (see above) were subcloned into the *XbaI-NdeI* sites of the pFAN9 vector by three-way ligation resulting in pFAN13. A 2.7 kb *XbaI-NdeI* fragment was isolated from pFAN13 and subcloned into the *XbaI-NdeI* sites of the pACXF vector resulting in pACXF-eGFP2A-17. Finally, an 8.1 kb *FseI-PacI* fragment was isolated from pBADFP and subcloned into the *FseI-PacI* sites of the pACXF-eGFP2A-17 vector resulting in pASD1-eGFP2A2.

pASD1-eGFP2A3 A 1 kb *SacI-AatII* cDNA fragment was amplified from viral RNA of ASD1-eGFP2A1-3 by RT-PCR using oligonucleotides BVD424 (5'-CAAACAAAAACCCGTCGG-3') and BVD1172 (5'-CTACGGCCAATATTGCC-3') and subcloned into the *SacI-AatII* sites of the pACXF vector resulting in pACXF-eGFP2A3. An 8.1 kb *FseI-PacI* fragment was isolated from pBADFP and subcloned into the *FseI-PacI* sites of the pACXF-eGFP2A3 vector resulting in pASD1-eGFP2A3.

***In vitro* transcription and transfection of MDBK cells**

cDNA plasmid (5 µg) was linearized with *SdaI* in a 100 µl reaction at 37°C, treated with proteinase K at 50°C for 30 min to degrade the restriction enzyme, extracted twice with phenol: chloroform (1:1), and precipitated twice with 2× ethanol and 10 µl of 3 M sodium acetate (pH 3.6). *In vitro* transcription was performed with 0.5 µg template and a T7-MEGAscript kit (Ambion) in a 20 µl system for 90 min at 37°C. Then 1 µl RNase-free DNase (Ambion) was added to degrade the DNA templates at 37°C for 20 min. The quality and quantity of the transcripts are determined by denaturing agarose gel electrophoresis and absorbance at 260 nm, respectively. For transfection, MDBK cells (60% confluent) were trypsinized, washed twice with ice-cold RNase-free phosphate-buffered saline (PBS) (AccuGene PBS, pH 7.4; Bio Whittaker, Rockland, Maine), and resuspended in PBS with a final concentration of 1×10^7 cell/ml. 5 µg of transcripts were added to 0.4 ml of cell suspension (4×10^6 cells), transferred to a 0.4 cm cuvette (Bio-Rad), and immediately pulsed twice with a Bio-Rad Gene Pulser (set at 1.3 kV, 25 µF and infinite resistance). Cells were allowed to recover on ice for 10 min before they were transferred into a 15 ml sterile tube for a 1:10 dilution with complete medium. Then, 0.1 ml of the 1:10 diluted transfected cells was used to determine the transfection efficiency in an infectious center assay (see below). The remainder of the cell suspension was seeded in a 25 cm² flask and incubated at 37°C. 72 hr post-transfection, viruses were harvested from the transfected cells by three freeze-thaw cycles and the virus titer determined in focus forming assay as described below.

Infectious center assay

The transfection efficacy of the infectious RNA was measured in an infectious center assay (Mendez, *et al.*, 1998). In detail, 6 hr before electroporation, each well of a 12-well plate was seeded with MDBK cells (3×10^5 /cell) in 0.5 ml medium. 0.1 ml of each of the 1:10 diluted transfected cells was added in the first row of the columns in a 12-well plate. A second 0.1 ml of each of the 1:10 diluted transfected cells was diluted serially in 1 ml complete medium and 0.1 ml of each of the dilutions was seeded into the second, third, and fourth row of the columns in the 12-well plate to provide serial 10-fold dilutions. Following 4 hr of incubation, the medium in each well of the plate was removed and the plate washed once with complete medium and the liquid medium replaced with an agarose overlay (0.3% Seakem LE agarose, FMC) in complete medium and incubated at 37°C. After 3 days, the agarose overlay was removed and the monolayer used for immunoperoxidase staining as described in focus forming assays (see below). The specific infectivity was expressed in focus forming units (FFU) per microgram of RNA.

Focus forming assay

MDBK cells (60% confluent) were infected with sequential 10-fold dilutions of virus. After 1 hr incubation at 37°C, the cells were washed twice with PBS (Bio Whittaker), supplied with fresh complete medium, and incubated at 37°C. 72 hr post-infection (p.i.), the monolayer was dried for 1.5 hr at room temperature, fixed with 3.7% formaldehyde for 10 min at room temperature and dried again for 1.5 hr at room temperature (RT). The cells were incubated at 37°C for 20 min with bovine polyclonal antiserum B224 (1/350 dilution in PBS-2% BSA). After washing twice with

PBS-Tween-20 (0.25% tween-20 in PBS), cells were incubated at 37°C for 20 min with peroxidase-conjugated goat anti-bovine IgG (1/300 dilution in PBS-2% BSA). Cells were then washed twice with PBS-Tween-20 and incubated with peroxidase substrate (Ambion) at room temperature for 25 min. The viral foci were viewed with a Leica light microscope.

Detection of genetic markers in recombinant viruses

MDBK cells (5×10^6) were seeded in a 75 cm² flask (Corning), incubated at 37°C for 2 hr, and infected with ASD1 at an MOI of 1.0 FFU/cell. After 60 hr incubation at 37°C, viral RNA was isolated as described above and RT-PCR was performed in a 50 µl volume using a Superscript™ one-step RT-PCR system with Platinum™ Taq DNA polymerase (Invitrogen, Carlsbad, CA) as described by the manufacturer. The RT step was performed for 1 hr at 45°C and the cDNA was then denatured for 2 min at 95°C and amplified by PCR for 45 cycles at 95°C for 1 min for template denaturing, 53°C for 45 sec for primer annealing, and 72°C for 2 min extension. The RT-PCR products were a 1662 bp fragment spanning the silent mutations T7575C and G7872C using primer pair BVD6891 and BVD7920, a 927 bp fragment spanning the silent mutation T9022A using primer pair BVD8905 and BVD9450, a 1170 bp fragment spanning the silent mutation A10912G using primer pair BVD9985 and BVD11155, and a 350 bp fragment spanning the point mutation A12264G using primer pair BVD12043 and SD1-SdaI-PacI (TABLE. 6). All cDNA products were confirmed by nucleotide sequencing.

Viral growth kinetics

For analysis of virus growth, monolayers of MDBK cells (~ 60% confluent) are infected with ASD1, ASD1-eGFP2A3, and wt SD1 at both a high MOI of 1.0 FFU/cell and a low MOI of 0.1 FFU/cell in wells of a 24-well plate. After 1 hr incubation, the

monolayer cells were washed twice with PBS and incubated at 37°C in fresh complete medium. At various time points p.i., progeny virions were collected and lysed by three freeze-thaw cycles and titered using the focus forming assay. In this study, one-step growth curves of the viruses were generated by plotting virus titers against time. The graphs show average values of virus titers derived from three independent experiments (Fig. 8).

Quantitative real time RT-PCR

To construct the nucleotide standard, BVDV-negative MDBK cells were incubated at 37°C for 72 hr. Total cellular RNA was extracted using a S.N.A.P total RNA isolation kit (Invitrogen, Carlsbad, CA), quantitated by spectrophotometer, and stored at -80°C in aliquots. Viral RNA from wt SD1 with a titer of 1.0×10^6 FFU/ml was serially diluted in 2.5 µg BVDV-negative total cellular RNA from MDBK cells to generate 1000, 100, 10, 1, 0.1, and 0.01 FFU of virus in a final volume of 10 µl. The virus-infected MDBK cells were collected at different time points p.i. Total cellular RNAs were isolated, quantitated, and stored at -80°C in aliquots as described above. Quantitative real time RT-PCR was performed on a LightCycler instrument (Roche, Mannheim, Germany) with a QuantiTect™ SYBR® green RT-PCR kit (Qiagen). The assay was performed in a 50 µl volume containing 2.5 µg of extracted RNA, a 1 µM concentration of either positive primer BVD424 or negative primer BVD764 (5'-TGCCGTCCTGCCAGTTA-3'), and the RT-PCR mix (Qiagen). The reactions were subjected to 42°C for 1 hr for RT, followed by 95 °C for 10 min to heat-inactivate reverse transcriptase and activate the HotStarTag DNA polymerase. After the RT step, the complementary primer was added to the reactions and the tubes were subjected to PCR amplification through 40 cycles of

95°C for 1 min, 57°C for 45 sec, and 72°C for 1 min. RNA was quantitated within the linear range of the assay and by reference to RNA extracted from a virus stock with a known titer.

Indirect immunofluorescence staining and flow cytometry

MDBK cells (1×10^5) were infected with wt SD1 or ASD1-eGFP2A3 at an MOI of 1.0 FFU/cell or mock-infected MDBK cells were used as a negative control. At different time points p.i., cells were collected by centrifugation at 1200 rpm for 2 min, washed twice with PBS, and fixed with 4% paraformaldehyde/PBS for 30 min at RT. The fixed cells were washed twice with PBS and incubated for 20 min at RT with anti-BVDV Mab D89 (1:300 dilution, VMRD, Pullman, WA), specific for the E2 protein of BVDV. Cells were washed twice with PBS, then further incubated with Alexa Fluor®680-conjugated rabbit anti-mouse IgG (H and L chains at 1:500 dilution, Molecular Probes, Eugene, OR) for 20 min at RT. After cells were washed twice with PBS, the fixed cells were resuspended in 0.3 ml PBS and analyzed by flow cytometry with following parameters: excitation wavelength 680 nm and detection wavelength 698 nm. The expression efficacy of the E2 protein was reflected by mean fluorescence intensity (MFI).

Visualization of the fluorescent cells

MDBK cells (1×10^4) were seeded in each well of a 4-well Lab-Tek chamber slide (Nunc, Rochester, NY), infected with wt SD1 or ASD1-eGFP2A3 at an MOI of 1.0 FFU/cell, and incubated at 37°C. At 60 hr p.i., the cell culture medium was removed and cells were fixed with 4% paraformaldehyde/PBS for 30 min at RT. The coverslips were washed twice with PBS, mounted on a slide using VECTASHIELD® HardSet™ mounting medium (Alexis, San Diego, CA), and viewed with an epi-fluorescence-

equipped Nikon Eclipse E600W microscope. Photos were captured using an RT-Slide Spot digital camera (Diagnostic Instruments, Sterling Heights, MI) at 200× amplification with an exposure time of 45 sec.

SDS-PAGE and immunoblotting

MDBK cells (1.5×10^6) were seeded in 25 cm² flasks (Corning), infected with either wt SD1 or ASD1-eGFP2A3 at an MOI of 1.0 FFU/ml. At different time points p.i., cells were washed twice with PBS and lysed in 300 μl of M-PER[®] Mammalian Protein Extraction Reagent (Pierce, Rockford, IL). Cell lysates were clarified twice at 10,000xg for 10 min and quantified by traditional BCA assay (Pierce) as described by the manufacturer. Cell lysates were separated on 8~16% SDS-PAGE (Precise protein gel, Pierce) with a loading of 40 μg protein per lane and transferred to an immobilon[™]-P PVDF membrane (Sigma-Aldrich, South San Francisco, CA). The membrane was blocked in 0.5% casein/PBS for 1h, incubated with BD living colors A.V. Mab JL-8 (1:1000 dilution in blocking buffer, Clontech, Palo Alto, CA) for 2 hr, washed three times with PBS followed by incubation with alkaline phosphatase-conjugated affinity purified goat antibody to mouse immunoglobulins (IgG, IgA, IgM) (1:1000 dilution in blocking buffer, MP Biomedicals, Aurora, OH) for 1 hr. After washing three times with PBS, eGFP2A protein was detected with alkaline phosphatase-conjugated substrate kit (Bio-Rad) for 10 min and recorded with a Canon Powershot A80 digital camera (Canon USA Inc, Lake Success, NY).

Flow cytometry of eGFP

To detect the expression of the eGFP2A protein, MDBK cells (1×10^5) were infected with wt SD1 or ASD1-eGFP2A3 at an MOI of 1.0 FFU/cell with mock-infected MDBK

cells as negative control. At the different time points p.i., cells were collected by trypsinization and centrifugation at 1200 rpm for 2 min, washed twice with PBS, and fixed with 4% paraformaldehyde/PBS at RT for 30 min. Following two washes with ice-cold PBS, the cells were resuspended in 0.3 ml PBS and the fluorescence of the cells was analyzed using a MoFlo 8-color flow cytometer & high-performance sorter (Dakocytomation) with the following parameters: excitation wavelength 488 nm and detection wavelength 525nm. The expression efficacy of the eGFP2A protein was reflected by the mean fluorescence intensity of the eGFP2A-positive cells.

RESULTS

Construction of a full length cDNA clone of BVDV SD1

In order to generate an infectious recombinant BVDV, we combined two strategies: (1) cloning the viral cDNA in a low copy number backbone of pACYC1180 to improve the stability of the cDNA clone in bacteria, and (2) using an *in vitro* transcription system to produce highly uniform transcripts. In this study, RT-PCR amplification was performed on viral RNA extracted from wt SD1 stock as described in the Materials and Methods section. Seven cDNA subclones, harboring cDNA fragments spanning the whole SD1 genome, were constructed using standard molecular biological methods. Nucleotide sequencing indicated that 6 coding point mutations, 4 noncoding point mutations, one single-nucleotide deletion and a four-nucleotide deletion were present in these subclones (TABLE 5). By site-directed mutagenesis, all the mutations and deletions except five noncoding point mutations, including T7575C, G7872C, G9022A, A10912G, and A12264G which served as genetic markers, were repaired and confirmed by nucleotide sequencing. The final resulting subclones were designated pSDXN1, pSDNF, pSDFN1, pSDNE2, pSDEN, pSDNN1 and pSDNP2, respectively. In pSDXN1, a T7 promoter sequence was designed into the oligonucleotide SD1-xbaI-T7 so that the T7 promoter sequence was abutted to the viral 5'-UTR by PCR amplification. Also, a *SdaI* site was designed into the oligonucleotide SD1-SdaI-PacI so that an *SdaI* site was attached immediately downstream of the 3'-UTR in pSDNP2 by PCR amplification. By

standard molecular methods, two plasmids, pACXF harboring the cDNA sequence of the 5' half of the SD1 genome (nt 1 to 4,204) and pBADFP containing the cDNA sequence of 3' half of the SD1 genome (nt 4,203 to 12,578) were constructed in pACNR1180 and pBADEH backbones, respectively. Finally, a full-length cDNA clone of BVDV strain SD1, pASD1, was established by inserting the 8.1 kb *FseI-PacI* fragment of pBADFP into the *FseI-PacI* digested pACXF vector. pASD1 has several characteristics including: a T7 promoter sequence immediately upstream of the SD1 genome for *in vitro* transcription; an engineered *SdaI* restriction site immediately downstream of the SD1 genome for linearization; and five noncoding mutations serving as genetic markers to distinguish it from the wt BVDV SD1 (Fig.1.).

Viable virus generated from the constructed cDNA clone

To determine whether the created viral construct was infectious, run-off transcripts were synthesized from *SdaI*-linearized pASD1 with T7 RNA polymerase and three independently-generated RNAs were electroporated into MDBK cells using the techniques described in Materials and Methods section. At 72 hr p.i., pASD1 was found clearly infectious with an average transfection efficiency of 4.5×10^5 FFU/ μ g RNA. Focus forming assay showed that the rescued virus, ASD1, approached a virus titer of 2.7×10^2 FFU/ml. After 6 additional passages, ASD1 was rescued and stocked as a working virus stock with a titer of 2.3×10^7 FFU/ml.

Detection of engineered genetic markers

To determine whether the rescued viruses originated from the constructed plasmids, ASD1 was used to infect MDBK cells at an MOI of 1.0 FFU/cell and viral RNA was extracted from the infected MDBK cells and analyzed by RT-PCR along with wt SD1

infected MDBK cells and Mock-infected MDBK cells as positive and negative controls, respectively. Using primer pairs flanking each of the genetic markers in ASD1, cDNA fragments with the sizes expected were obtained (data not shown), purified, and sequenced directly as described in Materials and Methods section. Sequencing data indicated that none of the genetic markers were present in wt SD1 genome, however, it was found that ASD1 contained all 5 noncoding mutations, namely, A5308T, T7575C, G7882C, G9022A, and A12264G (Fig. 2). Thus, this result demonstrated that the molecularly rescued virus, ASD1 was derived from the cDNA clone of pASD1.

Construction of a BVDV genome harboring an eGFP2A insert

The 17 amino acid peptide of foot-and-mouth disease virus (FMDV) 2A protease (FMDV 2A^{pro}) is an autoprotease which cleaves at its own C-terminus between a glycine-proline dipeptide independent of the presence of other viral sequences (Ryan, *et al.*, 1991, 1994; Percy, *et al.*, 1994). In this study, to develop a live-marked BVD virus, we inserted an in-frame eGFP gene between the N^{pro} and viral capsid (C) protein genes of BVDV so that the inserted eGFP gene was translated as part of the viral polyprotein which would subsequently be proteolytically cleaved to release separate N^{pro} protein, C protein, and eGFP protein. To achieve this, FMDV 2A^{pro} was fused in-frame to the C-terminus of eGFP to generate a fusion protein, eGFP2A, which provided the cleavage site at its C-terminus to release the C protein from the viral polyprotein. To ensure release of N^{pro} protein from the viral polyprotein by its own autocatalytic activity, a linker encoding an amino acid sequence of SDTKEVP was inserted in-frame between N^{pro} and eGFP2A to mimic the authentic N^{pro}/C junction by providing the cleavage motif of a cysteine-serine dipeptide (Stark, *et al.*, 1993). By this strategy, the final viral proteins generated

would be authentic N^{pro}, eGFP2A with additional 7 amino acids fused to its N-terminus, and C protein containing an additional N-terminal proline residue because of the intramolecular cleavage of FMDV 2A^{pro}. As described in Materials and Methods section, based on the full length infectious cDNA clone of BVDV strain SD1, pASD1, and the constructed plasmid, peGFP2A1, which harbors the nucleotide sequence coding for the eGFP2A protein, a cDNA clone termed pASD1-eGFP2A1 with a length of 13,587 base pairs was obtained (Fig. 3). In order to investigate whether the first N-terminal amino acid of C protein, a serine residue, could be replaced by other amino acids without interfering with virion assembly, we constructed another construct, pASD1-eGFP2A2 with a length of 13,584 base pairs in which the first amino acid, serine, of C protein was replaced by proline which came from the glycine-proline dipeptide by the intramolecular cleavage of FMDV 2A^{pro}. Nucleotide sequencing showed both pASD1-eGFP2A1 and pASD1-eGFP2A2 have the original sequence as engineered.

eGFP2A insertion was not stable in the recombinant viral genome

Using established techniques described in Materials and Methods section, each of three independently-generated viruses, derived from each of pASD1-eGFP2A1 and pASD1-eGFP2A2, were rescued in MDBK cells and designated as ASD1-eGFP2A1-1, ASD1-eGFP2A1-2, ASD1-eGFP2A1-3, and ASD1-eGFP2A2-1, ASD1-eGFP2A2-2, ASD1-eGFP2A2-3, respectively. RT-PCR of viral RNA was performed using primer pairs BVD424 and BVD1172, which span the eGFP2A insert in the recombinant viral genome. As shown (Fig. 4A and 4B), it was only ASD1-eGFP2A1-3 which demonstrated a unique cDNA fragment with the expected size of 1.5 kb while the other recombinant viruses showed three cDNA fragments in which two of them were found smaller than 1.5

kb. After an additional 5 passages, it was indicated that, except for ASD1-eGFP2A1-3 which still produced a unique cDNA fragment of 1.5 kb in size as expected, only the smallest cDNA fragment could be detected in the RT-PCR assay with the same primer pair (data not shown). Furthermore, nucleotide sequencing indicated that (Fig. 5C) only two point mutations, A1626G and A1627G, which resulted in an amino acid substitution of lysine, the C-terminal amino acid of eGFP to glycine, were detected in ASD1-eGFP2A1-3. However, large deletions and point mutations were found within the N^{pro}/eGFP2A junction in other recombinant viruses (Fig. 4). Taken together, eGFP2A sequence was not stable when inserted between the N^{pro} gene and the C gene of the BVDV genome. However, an eGFP2A insert harboring two adjacent point mutations, A1626G and A1627G, may contribute to its stabilization in viral genome. Considering that all the recombinant viruses can approach to a virus titer of $\sim 10^6$ FFU/ml at passage 10 (data not shown), it was concluded that different modifications of the N-terminal amino acid in C protein have the same effect or have no effect on the assembly efficiency of the recombinant virion.

A mutated eGFP2A sequence contributed to its stability in viral genome

To confirm whether the two point mutations in the eGFP2A insert contribute to its stabilization in the recombinant viral genome; pASD1-eGFP2A3 was constructed, based on pASD1-eGFP2A1, with the introduced point mutations of A1626G and A1627G (Fig. 1). The rescued virus, ASD1-eGFP2A3 derived from pASD1-eGFP2A3, was passaged 10 times and stocked as working virus stock with a titer of 2.7×10^6 FFU/ml. RT-PCR of viral RNA isolated from ASD1-eGFP2A3 at passage 0 and 10 was performed using two primer pairs, BVD424+BVD1172 and BVD687 (5'-CCCCACTGGAGCTCTTTG-3')

+BVD1172 which span the eGFP2A insertion in the recombinant viral genome. As shown in Fig. 5, cDNA fragments with the expected size of 1.5 kb and 1.3 kb were detected from ASD1-eGFP2A3 at both passage 0 and passage 10 using two primer pairs, respectively. Furthermore, nucleotide sequencing confirmed that the introduced point mutations were present exactly in the original sites of the eGFP2A insertion as engineered (Fig. 5) and no other mutations or deletions were detectable within the eGFP2A insertion, the eGFP2A/C junction, or the N^{pro}/eGFP2A junction. Consequently, these results demonstrated that ASD1-eGFP2A3 retained the original sequence of the cDNA clone, pASD1-eGFP2A3 and that the mutated eGFP2A insert had been stably retained in the viral genome of ASD1-eGFP2A3 for at least 10 passages.

Viral replication of ASD1-eGFP2A3 comparable to that of wt SD1

Using the methods described in Material and Methods section, SYBR-green quantitative real time RT-PCR was performed to compare viral RNA replication of ASD1-eGFP2A3 to that of wt SD1 in a time course analysis. MDBK cells were infected with ASD1-eGFP2A3 and wt SD1 at an MOI of 1 FFU/ml and incubated at 37°C. At 12 hr, 36 hr, and 60 hr post-infection, total cellular RNA from ASD1-eGFP2A3-infected or wt SD1-infected-MDBK cells was extracted and positive or negative primer was selectively used in RT step and the complementary primers were added after the RT-step to allow quantitative real time PCR amplification. As shown in Fig. 6, accumulation of both positive viral RNA and negative RNA of ASD1-eGFP2A3 was almost identical to that of wt SD1 at all indicated time points and the expression level of the positive viral RNA of ASD1-eGFP2A3 was nearly 100 times higher than that of the negative viral RNA at any indicated time points.

Next, viral glycoprotein E2, the primary antigenic epitope of BVDV, was selected as a target for comparison of viral protein expression between ASD1-eGFP2A3 and wt SD1. MDBK cells were infected with ASD1-eGFP2A3 and wt SD1 at an MOI of 1 FFU/ml and incubated at 37°C. At 60 hr post-infection, cells were labeled by indirect immunofluorescence and analyzed by flow cytometry as described in Materials and Methods section. As shown in Fig. 7, both of the viruses had mean fluorescence intensity (MFI) of ~21 for E2 expression, however, as negative controls, the mock-infected MDBK cells only had a MFI of ~1.28, one eighteenth the fluorescence level compared to that of the viral infected samples. Thus, it was concluded that E2 protein expression of ASD1-eGFP2A3 was completely comparable to that of wt SD1. In summary, it was demonstrated that the eGFP2A insert between the N^{pro} gene and C gene of BVDV did not interfere with RNA replication and protein expression of the recombinant virus to the limits of detection.

Single step viral growth analysis

To investigate whether the eGFP2A insertion interfered with viral maturation, growth properties of ASD1-eGFP2A3 and wt SD1 were compared after infection of MDBK cells at both a high (1.0FFU/ml) and a low (0.1 FFU/ml) multiplicity of infection. As shown in Fig. 8, it appeared that the replication kinetics of ASD1-eGFP2A3 and wt SD1 were similar at both MOIs and both of the viruses approached a maximum virus yield at approximately 60 hr post-infection although the peak titer of ASD1-eGFP2A3 was approximately 0.5 log₁₀ lower than that of wt SD1 and the maximum virus yield was around 4 hr later than that of wt SD1. Considering that the eGFP2A insert did not interfere with RNA replication and protein expression of ASD1-eGFP2A3 as described

above, it was hypothesized, together with this result that maturation of the infectious recombinant virus was interfered slightly with either by the eGFP2A insert between the N^{pro} gene and C gene of the recombinant viral genome, or by the altered C protein containing an additional N-terminal proline residue because of the intramolecular cleavage of FMDV 2A^{pro}, or both. Alternatively, it is also possible that synthesis of the additional eGFP2A protein imposed a sufficiently large metabolite burden that it competed with or slowed viral replication in some manner.

eGFP2A protein was generated properly during viral polyprotein processing

To examine the expression and accumulation of functional eGFP2A protein, MDBK cells were infected with ASD1-eGFP2A3 or wt SD1 at an MOI of 1.0 FFU/ml and incubated at 37°C. At 12 hr, 36 hr, and 60 hr post-infection, respectively, cells were fixed and analyzed by flow cytometry as described in Material and Methods section. As indicated (Fig. 9), fluorescence in ASD1-eGFP2A3-infected MDBK cells can be detected as early as 12 hr post-infection, and increased with time to a peak at approximately 60 hr post-infection. The MFI of ASD1-eGFP2A3-infected MDBK cells at 12 hr, 36 hr, and 60 hr post-infection was approximately 1.12, 13.87, and 20.32 times brighter, respectively, than that of negative controls. These results indicated that the eGFP2A protein was not only expressed and was functional in ASD1-eGFP2A3-infected MDBK cells but also accumulated to a high level at 60 hr post-infection. To confirm whether eGFP2A protein was being cleaved properly during viral polyprotein processing, western blotting was performed in a time course analysis as described in Materials and Methods section. As shown (Fig. 10), although eGFP2A protein was undetectable at 12 hr post-infection, one unique band with a molecular mass of ~30 kDa, corresponding to the size of eGFP2A

protein, was detected in ASD1-eGFP2A3-infected MDBK cells at 24 hr post-infection and approached a maximum yield at 60 hr post-infection. This result demonstrated that eGFP2A protein was cleaved properly in ASD1-eGFP2A3-infected MDBK cells as engineered. In summary, eGFP2A protein was expressed as part of the viral polyprotein and cleaved completely from the precursor viral polyprotein in ASD1-eGFP2A3-infected MDBK cells to yield a mature and functional 30 kDa eGFP2A protein. Also, expression of eGFP2A in ASD1-eGFP2A3-infected MDBK cells was stable for at least 60 hr post-infection.

eGFP2A protein was localized to the cytoplasm and maintained stably in MDBK cells over multiple cell passages

To determine whether eGFP2A protein could be detected directly in host cells infected with ASD1-eGFP2A3, MDBK cells were cultured on glass chamber slides, infected with ASD1-eGFP2A3 at an MOI of 1 FFU/ml, incubated for 60 hr at 37°C, and examined by fluorescence microscopy as described in Materials and Methods section. As shown (Fig. 11A), the fluorescence was robust enough to be readily detected in ASD1-eGFP2A3-infected MDBK cells and the fluorescence signal was found evenly distributed in the cytoplasm and excluded from the nuclei of the host cells as expected. To examine whether eGFP2A protein could be maintained stably in persistently-infected host cells, MDBK cells were infected with ASD1-eGFP2A3 at an MOI of 1 FFU/ml and passaged continuously for 30 days (10 passages). Following trypsinization and passage, no cell death or cytopathogenic effects on host cells were observed (data not shown). As assayed by fluorescence microscope, equivalent intensity of fluorescence was detected in persistently-infected MDBK cells at passage 1 (3 days post-infection), passage 5 (15 days

post-infection), and passage 10 (30 days post-infection), respectively (Fig. 11B).

Consequently, these results indicate that eGFP2A protein was robust enough to be detected directly by fluorescence microscopy. Furthermore, eGFP2A protein was not toxic to host cells and could be maintained in host cells stably over time for at least 10 cell passages.

TABLE 1. Oligonucleotides used for nucleotide sequencing

Oligonucleotides	Nucleotide Sequence	Polarity	Nucleotide position*
M13 forward	5'-TCCCAGTCACGACGTCGT-3'	+	N/A
M13 reverse	5'-GGAAACAGCTATGACCATG-3'	-	N/A
BVD424	5'-CAAACAAAAACCCGTCGG-3'	+	424-441
BVD764	5'-TGCCGTCACCTGCCAGTTA-3'	-	747-764
BVD875	5'-TGGGTCACAAGCTGCTCA-3'	+	875-892
BVD1155	5'-GGGCAATATTGGCCGTAG-3'	+	1155-1172
BVD1739	5'-CTTGTTGACGGGGTGACC-3'	+	1739-1756
BVD1991	5'-ACCAATGCAGAGGATGGC-3'	+	1991-2008
BVD2309	5'-CCTGACCCACCTCTTCGA-3'	-	2292-2309
BVD4734	5'-GAAATGAGACCGTGGCCG-3'	+	4734-4751
BVD5044	5'-TTGCCCCCTAGCGGTATA-3'	-	5027-5044
BVD5830	5'-AGCAACAGGGGCAGGAAA-3'	+	5830-5847
BVD6314	5'-GCGGGGCTAAAAATCCCC-3'	+	6314-6331
BVD6891	5'-AATCCAGTCCCCCAGCTG-3'	+	6891-6908
BVD7386	5'-AGGAATTGGCGTCGGGCG-3'	+	7386-7403
BVD7875	5'-AAGTGGTGGAACCGGCC-3'	+	7875-7892
BVD8313	5'-ACAAGGGCTGGGAGGCCA-3'	+	8313-8330
BVD8905	5'-TACTGGGGTCGGGTTCG-3'	+	8905-8912
BVD9555	5'-TGATGGCAGAAGGGCGCA-3'	+	9555-9572
BVD10592	5'-AGCCTGCGGCCCTTCC-3'	-	10575-10592
BVD11155	5'-ACTTGTGTCTGGCTGGCC-3'	-	11138-11155
BVD11598	5'-ACAAGCGGGTTCAGGAA-3'	-	11581-11598
BVD12084	5'- TCTCAGCTGCTGGCGCCG -3'	-	12067-12084

* Nucleotide positions with reference to the published sequence of BVDV SD1 (Genbank Accession No. M96751)

N/A means the primers are not located inside the genome sequence of BVDV SD1.

TABLE 2. Oligonucleotides and template plasmids used for site-directed mutagenesis

Mutations	Template plasmids	Oligonucleotides*
G1472A	pSDXN	5'-CCTTGGATTTTAATCATGAATAGAA-3' 5'-TTCTATTCATGATTTAAAATCCAAGG-3'
A6278G	pSDNE	5'-CCCGAGGTGATGGAAGGGGAAGATC-3' 5'-GATCTTCCCCTTCCATCACCTCGGG-3'
T6858A	pSDNE1	5'-TGCTAATAACCCAGTTAGAAATACT-3' 5'-AGTATTTCTAACTGGGTAAAAGCA-3'
G8748T	pSDNN	5'-ATGATGATAATCTCAGAGAGATAAG-3' 5'-CTTATCTCTCTGAGATTATCATCAT-3'
C10583G	pSDNP	5'-AACAGGAAAGGGGCCGAGGCTTCC-3' 5'-GGAAGCCTGCGGCCCTTTCCTGTT-3' 5'-GCCAGCAGCTGAGACAAAATGTAT
A12089	pSDNP1	ATATTATAAATAG-3' 5'-CTATTTATAATATATACATTTTGTCTCA GCTGCTGGC-3' 5'-GGCAGAAGGCACAGAAAACTTC
ACTT 4455-4458	pSDEN	TCCATGCTTTTGCC-3' 5'-GGCAAAAGCATGGAGAAGTTTTTCTGT GCCTTCTGCC-3' 5'-GAGTGCACCATATTCGGTGT
G183T	pUCEH	GAAATACC-3' 5'-GGTATTTACACCGAATATGG TGCACTC-3'

* The bold nucleotides represent the corrected nucleotides with the position listed in the volume of "mutations".

TABLE 3. Oligonucleotides used for synthesis of subcloning adaptors

Primers	Nucleotide Sequence*
PUCPOSF	5'-ACGCCTVTAGACTCGAGCTCCGGACCG GCCGGCCATGCATTAATTAA-3'
PUCNEGF	5'- AGCTTTAATTAATGCATGGCCGGCCGGT CCGGAGCTCGAGTCTAGAGG-3'
PUCEHP	5'- AATTCATGCATTAATTAATGTACACTAGTGGTACCATATGGAT CCTGCAGAGCTCGGCCGCCGGGCTCGAGCCATGGCCGGCCA-3'
PUCEHN	5'- AGCTTGGCCGGCCATGGCTCGAGCCCGGGCGGCCGAGCTCTG CAGGATCCATATGGTACCACTAGTGTACATTAATTAATGCATG-3'

* The oligonucleotides were annealed to provide cloning adaptors with restriction enzyme sites for subcloning and cloning.

TABLE 4. Oligonucleotides used for construction of the subclones

cDNA position	Oligonucleotides*	Polarity	Resulting Plasmid
1-1916	SD1-XbaI-T7 5'- <u>CCGGTCTAGATAAT</u> <u>ACGACTCACGTATACGAGA</u> ACTAG-3'	+	pSDXN
	BVD 2094 5'-GCCGTTTCTGGTGCAAAG-3'	-	
1917-4209	BVD1793 5'-CTTGTTGACGGGGTGACC-3'	+	pSDNF
	4636L18 5'-TCCATGGACCAATTCAGC-3'	-	
4210-6037	4190U18 5'-TGGAAGATTGACTTGGCC-3'	+	pSDFN
	BVD6374 5'-TCGTGGGCACGAAAACCA-3'	-	
6038-6900	BVD5830 5'-AGCAACAGGGGCAGGAAA-3'	+	pSDNE
	BVD6951 5'-TGGATCGGCTCTGGGTGA-3'	-	
6901-8461	BVD6891P 5'-AAGACTTGCCGGCCGCTG-3'	+	pSDEN
	BVD8523N 5'-GCAGGGGCCCATCCCAGT-3'	-	
8462-10126	BVD8313P 5'-ACAAGGGCTGGGAGGCCA-3'	+	pSDNN
	BVD10545N 5'-CGTGGGAGCAACTTGAGG-3'	-	
	BVD9985P 5'-GCTGTTACGGTGCCCCGCC-3'	+	
10127-12319	SD1-SdaI-PacI 5'- <u>AGTTAATTAACCTGCAGG</u> GGGCTGTTAGAGG-3'	-	pSDNP

* The underlined nucleotides means a *XbaI* site followed by a T7 promoter sequence in SD1-XbaI-T7 and a *PacI* site followed by an *SdaI* site in SD1-SdaI-PacI.

TABLE 5. Comparison between the viral cDNA subclones and original SD1 genome

Nucleotide position	Type of mutation	Subclone location	Gene location
A1472G	coding	pSDXN	E ^{ns}
G6278A	coding	pSDNE	NS3
A6858T	coding	pSDNE	NS3
T7575C	noncoding	pSDEN	NS4A
G7872C	noncoding	pSDEN	NS4A
T8748G	coding	pSDNN	NS5A
G9022A	noncoding	pSDNN	NS5A
G10583C	coding	pSDNP	NS5B
A10912G	noncoding	pSDNP	NS5B
12089	single-nucleotide deletion	pSDNP	NS5B
A12264G	noncoding	pSDNP	3'-UTR
4455-4458 ACTT	Four-nucleotide deletion	pSDEN	NS2

TABLE 6. Oligonucleotides used for detection of the genetic markers in ASD1

Size of RT-PCR Products	Oligonucleotides	Polarity	Oligonucleotides position*
1.2 kb	BVD6891 5'-AAGAAGACTTGC CGGCCGCTG-3'	+	6891-6911
	BVD7920 5'-GCGCTGGTGGCA TAGGGG-3'	-	7902-7920
500 bp	BVD8905 5'-TACTGGGGTCGG GTTCCG-3'	+	8905-8913
	BVD9450 5'-GGCCTCGCGTCC TTGTTG-3'	-	9432-9450
1.1 kb	BVD9985 5'-GCTGTTCCGGTG CCCGCC-3'	+	9985-10003
	BVD11155 5'-ACTTGTGTCTG GCTGGCC-3'	-	11137-11155
550 bp	BVD12043 5'-AAAGGTCCTG CTCATGGC-3'	+	12043-12061
	SD1-SdaI-Pac 5'-AGTTAATTAACCT GCAGGGGGCTGTTAGAGG-3'	-	12565-12578

* Nucleotide positions with reference to the published sequence of BVDV SD1 (Genbank Accession No. M96751)

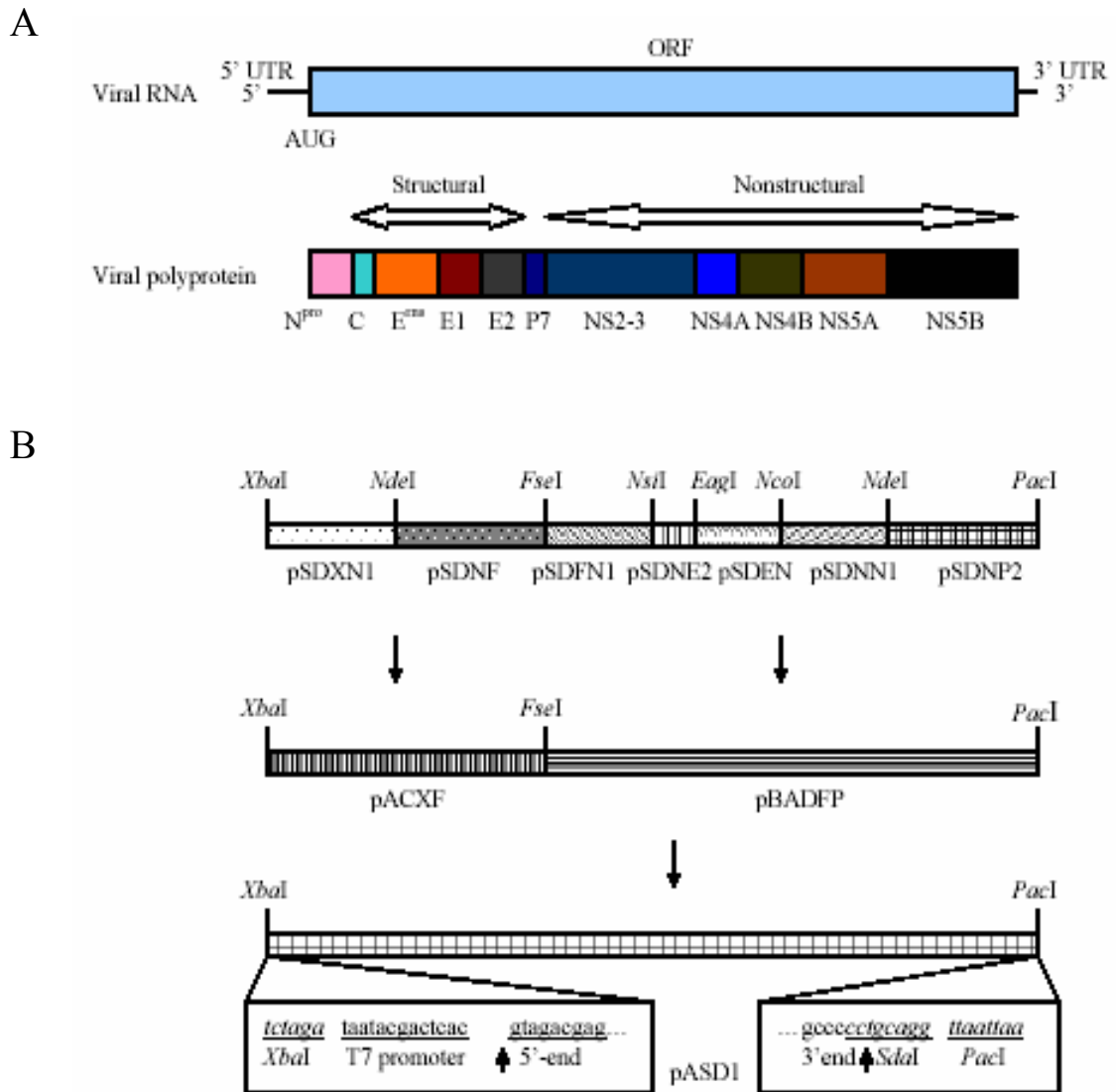


Fig. 1 Construction of a full-length cDNA clone of BVDV SD1. (A) Schematic representation of the RNA genome of BVDV SD1. The BVDV SD1 genome is a linear positive-polarity RNA of 12,809 nucleotides including a 5'-UTR of 385 nt, a large ORF of 12,242 nt, and a 3'-UTR of 285 nt. The bar at the bottom indicates the position and approximate size of the viral proteins in the polyprotein sequence. (B) Subclones used in the assembly of a full-length SD1 BAC cDNA clone. The sequence shown below include: the T7 promoter sequence (lowercase and underlined), engineered run-off restriction site of *SdaI* (italic lowercase, underlined). The restriction sites and plasmids used for subcloning are marked.

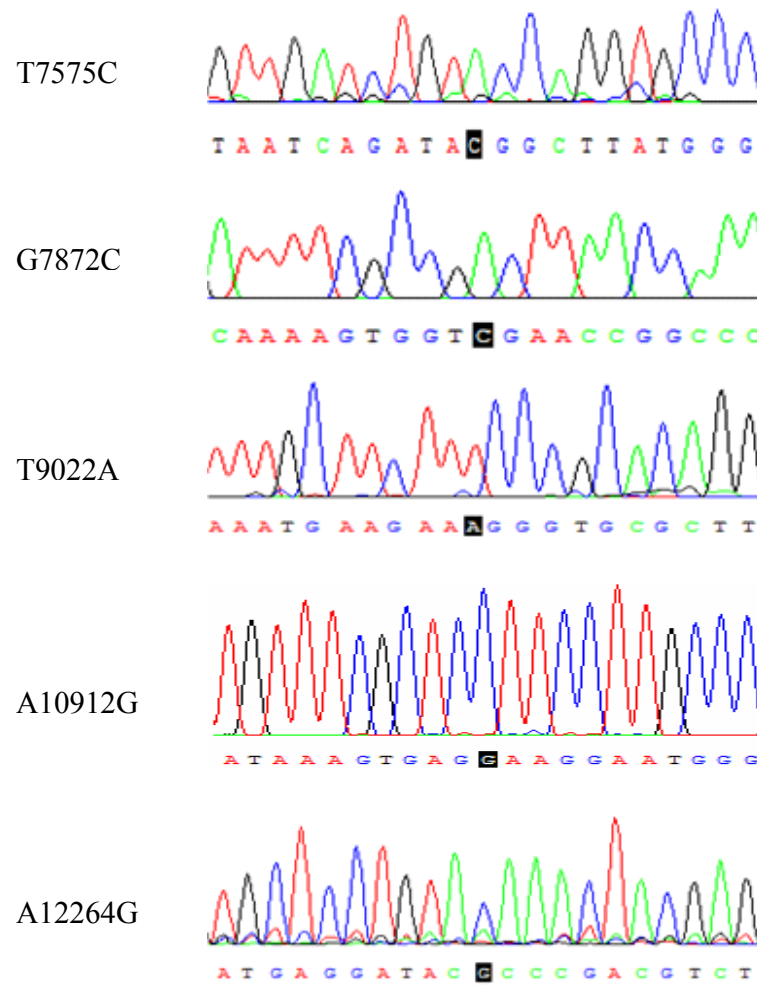


Fig. 2 Identification of the genetic markers in ASD1. The RT-PCR amplification of the total cellular RNA extracted from ASD1-infected MDBK cells was performed using primer pairs which span the genetic markers in the viral genome of ASD1. The obtained cDNA fragments were purified and sequenced as described in Materials and Methods section. Portion of the sequencing data are shown and the listed mutations are as follow: T7575C; G7872C; T9022A; A10912G; and A12264G. The point mutations are indicated in bold in each panel.

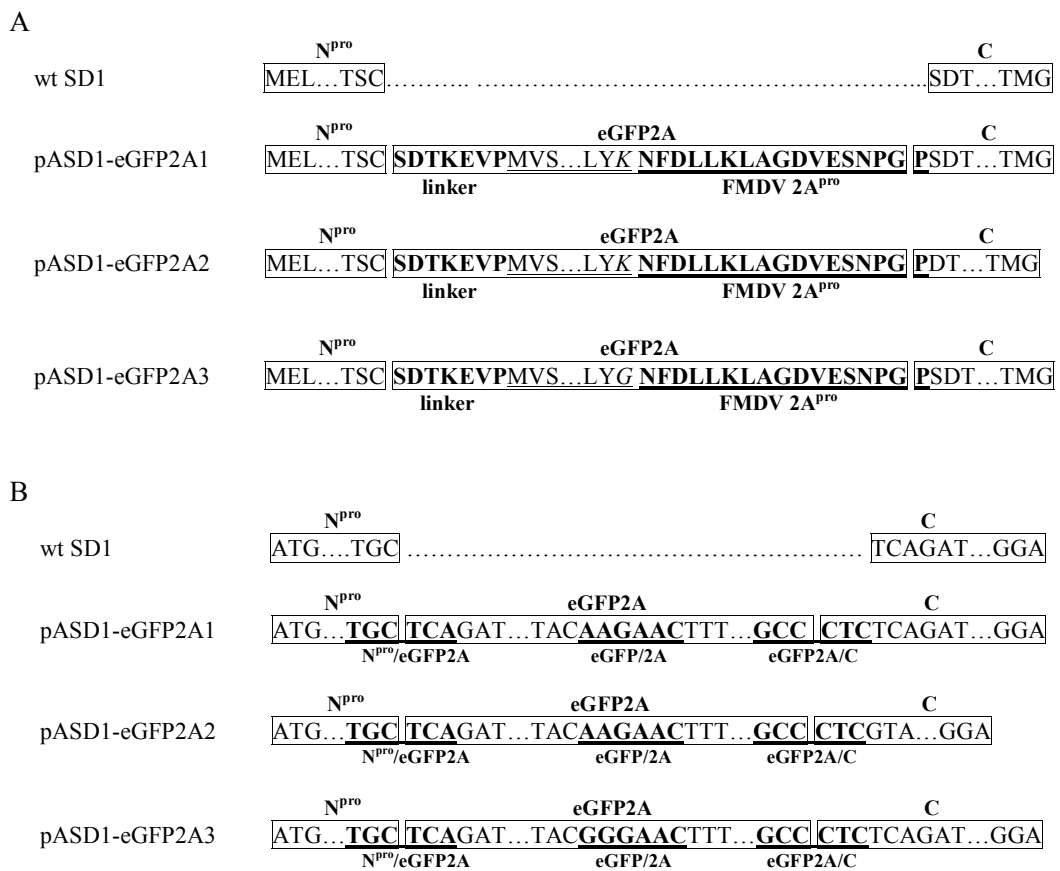


Fig. 3 Construction of cDNA clones of BVDV SD1 with the eGFP2A insert between the N^{pro} gene and the viral capsid (C) protein gene. (A) Schematic representation of part of the amino acid sequences deduced from wt SD1, pASD1-eGFP2A1, pASD1-eGFP2A2, and pASD1-eGFP3. The amino acids encoded by the N^{pro}, eGFP2A, and C genes are marked with boxes. The 7 amino acid linker peptide is marked with bold. The amino acids of eGFP are underlined. The 17 amino acid peptide of FMDV 2A^{pro} is marked with both bold and underline. The italics amino acid represents that substitution of K to G in pASD1-eGFP2A3. (B) Schematic representation of part of the nucleotide sequence of wt SD1, pASD1-eGFP2A1, pASD1-eGFP2A2 and pASD1-eGFP2A3. The nucleotide sequence coding for the N^{pro}, eGFP2A, and C genes are marked with boxes. Both underlines and bold are used to represent the N^{pro}/eGFP2A, eGFP/2A, and eGFP2A/C junctions.

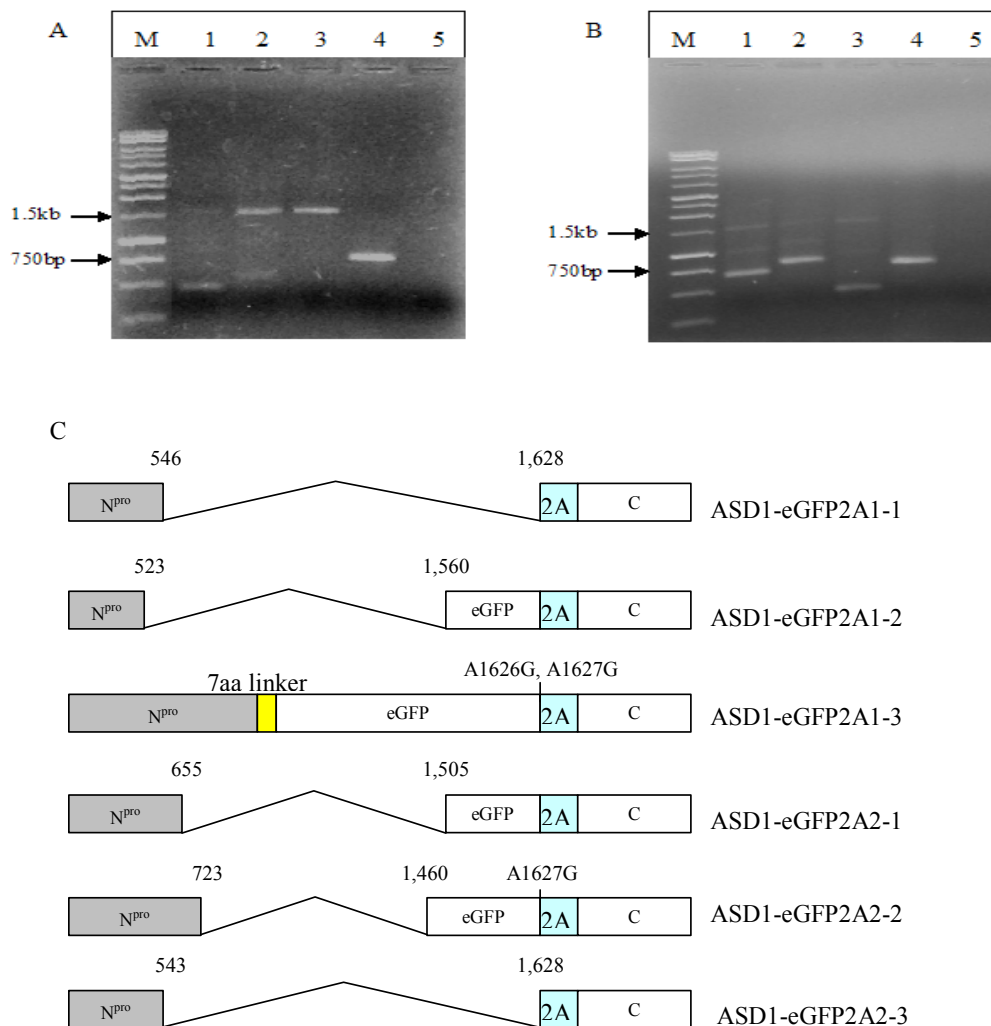


Fig. 4 The original eGFP2A insert is not stable in the recombinant viral genome. cDNA fragments amplified from the viral RNA of ASD1-eGFP2A1 (A) and ASD1-eGFP2A2 (B) by RT-PCR. Oligonucleotides used for RT-PCR were BVD424 and BVD1172. For both panels A and B, M: 1 kb DNA ladder; Lane 1 to Lane 3: cDNA fragments amplified from viral RNAs of ASD1-eGFP2A1-1, ASD1-eGFP2A1-2 and ASD1-eGFP2A1-3 (A) or ASD1-eGFP2A2-1, ASD1-eGFP2A2-2, and ASD1-eGFP2A2-3 (B); Lane 4: cDNA fragment amplified from viral RNA of wt SD1 as a positive control; Lane 5: blank reaction with no viral RNA template as a negative control. (C) Comparison of the nucleotide sequences of partial recombinant viral genomes with different deletions at the N^{pro}/eGFP2A junction. ASD1-eGFP2A1-1, ASD1-eGFP2A1-2, and ASD1-eGFP2A1-3 were derived from pASD1-eGFP2A1 independently. ASD1-eGFP2A2-1, ASD1-eGFP2A2-2, and ASD1-eGFP2A2-3 were generated from pASD1-eGFP2A2 independently.

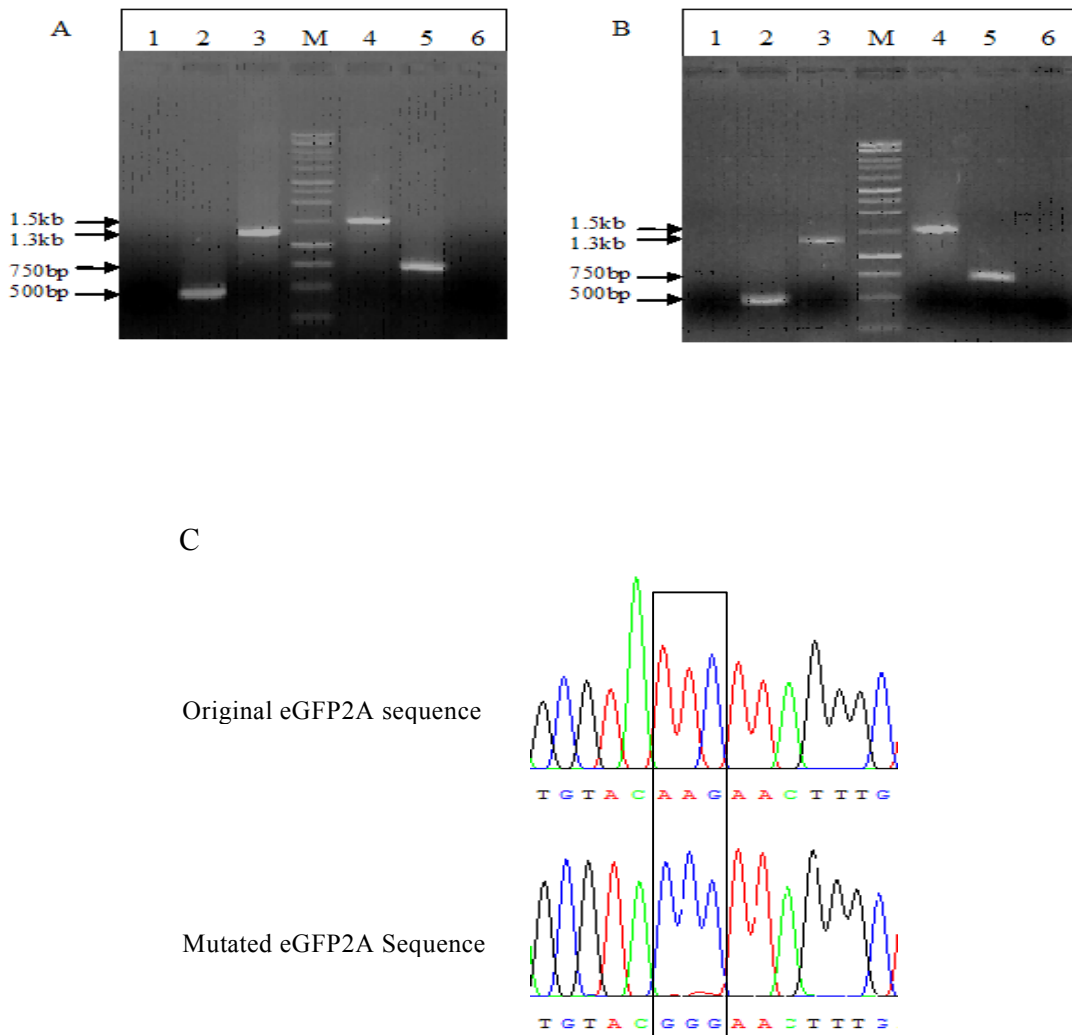


Fig. 5 The mutated eGFP2A insert is stable in the recombinant viral genome. cDNA fragments amplified from viral RNA of ASD1-eGFP2A3 at passage 0 (A) and at passage 10 (B) by RT-PCR. For both panel (A) and (B), M: 1 kb DNA ladder; Lane 1 and Lane 6: blank reaction as negative control; Lane 2 and Lane 5: cDNA fragments amplified from viral RNA of wt SD1 as positive control; Lane 3 and Lane 4: cDNA fragments amplified from viral RNA of ASD1-eGFP2A3. Oligonucleotides used for RT-PCR were either BVD687 plus BVD1172 (Lane 1, Lane 2 and Lane3) or BVD424 plus BVD1172 (Lane 4, Lane 5 and Lane 6). (C) Point mutations of A1626G and A1627G in the eGFP2A insert. Partial nucleotide sequences from original and mutated sequence of eGFP2A are compared.

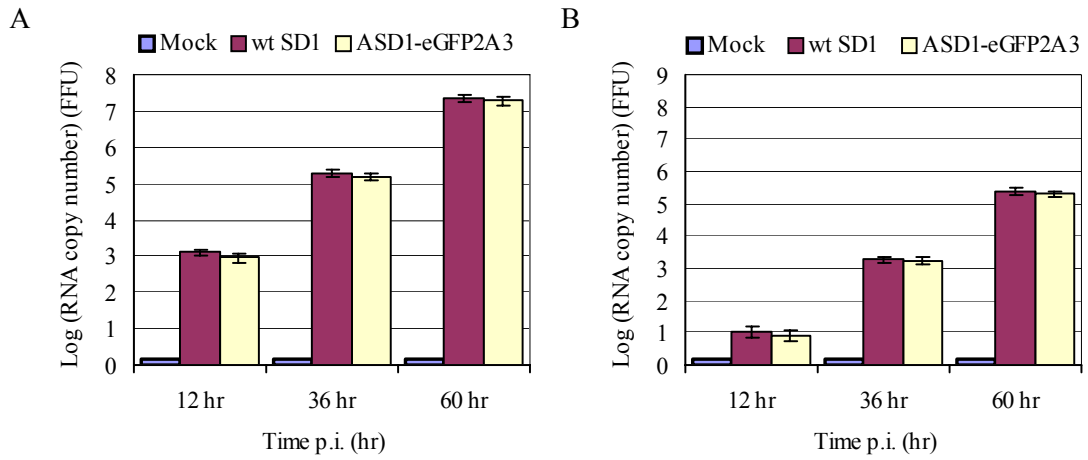


Fig. 6 eGFP2A insert does not interfere with the recombinant viral RNA replication. SYBR-green quantitative real time RT-PCR assay of viral RNA replication in a time course analysis (A) Quantitation of viral positive-strand RNA and (B) Quantitation of viral negative-strand RNA. For both panels (A) and (B), MDBK cells were infected with wt SD1 or ASD1-eGFP2A3 at an MOI of 1.0 FFU/cell. Cells were harvested at indicated time points p.i., total cellular RNAs were isolated, and viral positive and negative RNA was estimated. Here, total cellular RNA extracted from BVDV-negative MDBK cells were set as the negative control and the error bars represent the standard deviation.

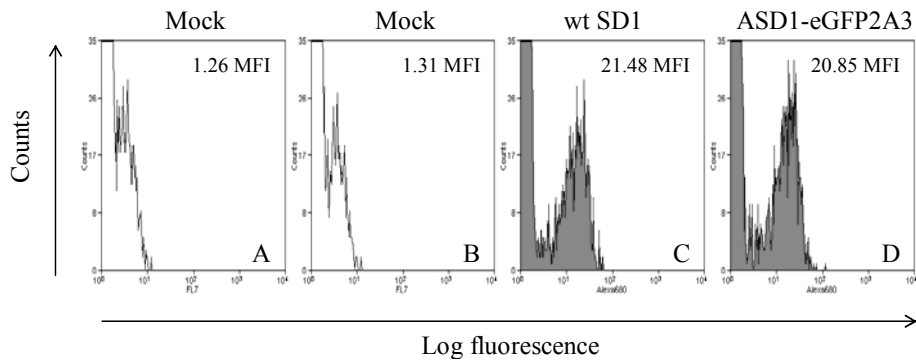


Fig. 7 eGFP2A insert does not interfere with the recombinant viral protein expression. MDBK cells were infected with ASD1-eGFP2A3 and wt SD1 at an MOI of 1 FFU/cell as well as mock-infected MDBK cells as negative control (mock). At 60 hr post-infection, cells were collected by trypsinization and centrifugation, washed twice with PBS, and fixed with 4% paraformaldehyde/PBS followed by indirect immunofluorescence staining (IFA) with Mab D89 against viral E2 protein as the primary antibody and Alexa Fluor®680-conjugated rabbit anti-mouse IgG (H+L) as the secondary antibody. The fluorescence intensity of the cells was determined by flow cytometry as described in Materials and Methods with a detection spectrum of 698 nm. The expression efficacy of viral E2 protein was reflected by the mean fluorescence intensity (MFI) of the E2-positive cells indicated inside the panels.

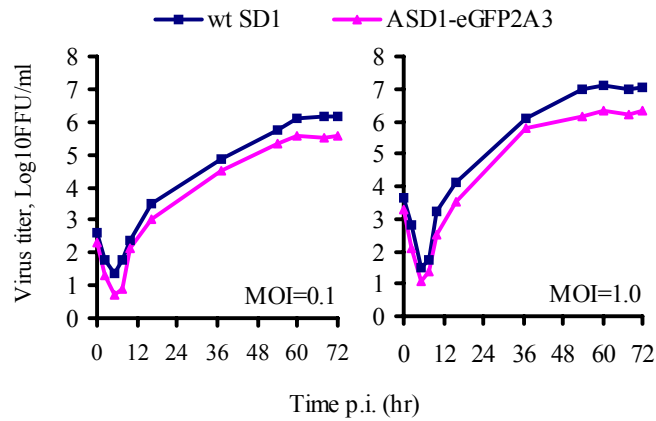


Fig. 8 Comparison of viral growth kinetics between ASD1-eGFP2A3 and wt SD1. MDBK cells were infected with viruses at an MOI of either 0.1 FFU/cell or 1 FFU/cell in triplicate in 24-well plates. At the different time points indicated, cells were collected by trypsinization and centrifugation, washed twice with PBS, and lysed by three cycles of freeze-thaw. Viral titers were determined by focus-forming assays as described in Materials and Methods section. One-step growth curves of the viruses were generated by virus titers plotted against time. The graphs show average values of virus titers derived from three independent experiments.

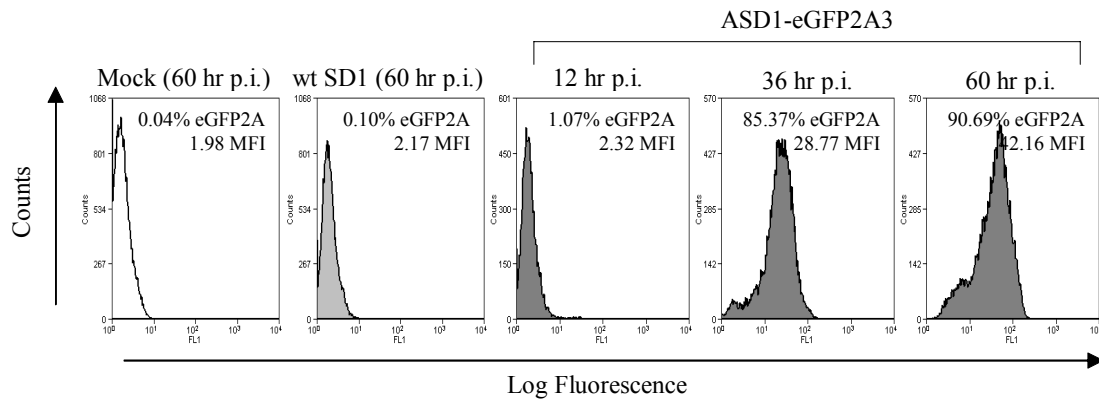


Fig. 9 eGFP2A protein is expressed in ASD1-eGFP2A3-infected MDBK cells. MDBK cells were infected with ASD1-eGFP2A3 at an MOI of 1.0 FFU/cells as well as MDBK cells infected with wt SD1 at an MOI of 1.0 FFU/cell and mock-infected MDBK cells (Mock) as negative controls. At 12 hr, 36 hr, and 60 hr post-infection as indicated, cells were fixed and analyzed by flow cytometry with a detection spectrum of 525 nm as described in Materials and Methods section. The percentage of the fluorescence-positive cells (eGFP2A) is indicated inside each panel. eGFP2A protein expression was indicated by mean fluorescence intensity (MFI) of the eGFP2A-positive cells as shown inside each panel.

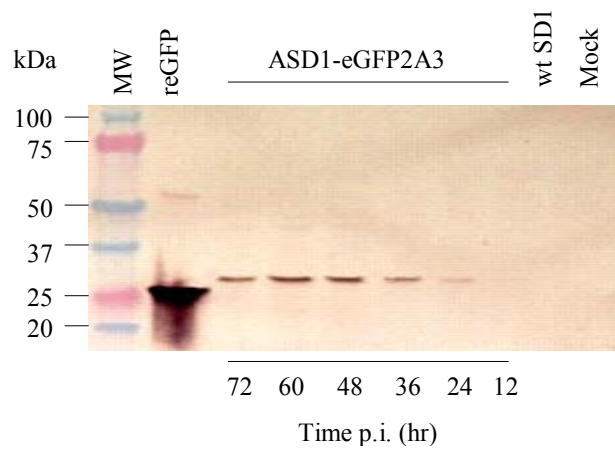


Fig. 10 eGFP2A protein is processed properly in ASD1-eGFP2A3-infected MDBK cells. MDBK cells infected with ASD1-eGFP2A3 at an MOI of 1.0 FFU/cell as well as MDBK cells infected with wt SD1 at an MOI of 1.0 FFU/cell and mock-infected MDBK cells (Mock) as negative controls. At the different time points indicated, cells lysates were separated by 6~18% sodium dodecyl sulfate-polyacrylamide gel electrophoresis (SDS-PAGE), followed by western blotting and reaction with Mab JL-8 against eGFP2A protein. For each lane, a total 40 μ g cellular protein was loaded. Lane 1. Molecular mass standard in kilodaltons (indicated on the left); Lane 2. 15 ng of recombinant GFP protein as positive control; Lane 3 to Lane 8. Cell lysates of ASD1-eGFP2A3-infected MDBK cells at different time points p.i. as indicated; Lane 9 and lane 10. cell lysates of wt SD1-infected MDBK cells and mock-infected MDBK cells, respectively, as negative controls.

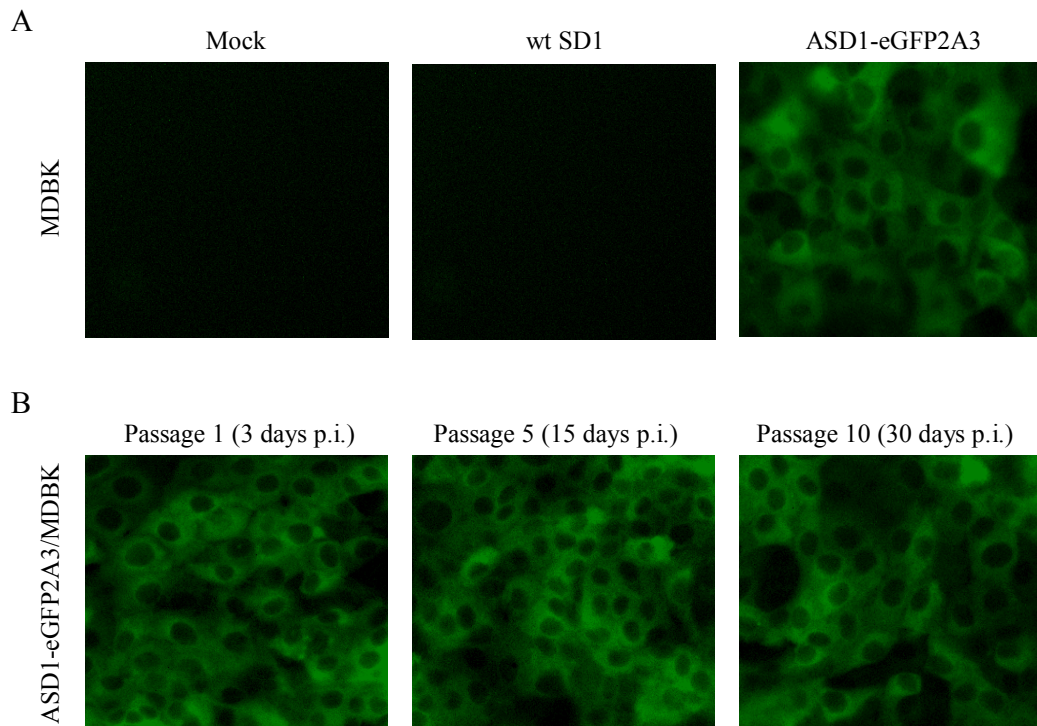


Fig. 11 eGFP2A was maintained stably in ASD1-eGFP2A-infected MDBK cells. MDBK cells were infected with ASD1-eGFP2A3 at an MOI of 1 FFU/cell as well as MDBK cells infected with wt SD1 at a MOI of 1.0 FFU/cell and mock-infected MDBK cells (Mock) as negative controls. Cells were visualized at 200X amplification as described in Materials and Methods section. Images were captured with an exposure time of 45 sec. (A) MDBK cells were fixed at 60 hr post-infection. Mounting media was added to the chamber slides and sealed. (B) ASD1-eGFP2A3-infected MDBK cells were passaged once every three days for 30 days (10 passages). MDBK cells from 1st passage, 5th passage and 10th passage were fixed at 60 hr p.i.

DISCUSSION

Reverse genetics of single-stranded, plus-sense RNA viruses have provided a powerful tool to investigate nearly all aspects of the viral life cycle and pathogenesis by constructing infectious full length cDNA clones (Rice, *et al.*, 1987; Davis, *et al.*, 1989). In this study, based on the infectious cDNA clone, pASD1 of NCP type-I BVDV strain SD1, we succeeded in generating a live-marked recombinant BVD virus, ASD1-eGFP2A3, from which the eGFP2A protein, a fusion protein of eGFP and FMDV 2A^{pro} was expressed properly and maintained stably in MDBK cells. Considering the biological background and the advantages of the playing wt SD1 in animal testing (Deng & Brock, 1992), ASD1-eGFP2A3 should provide a very useful tool as a real time monitoring system to elucidate the mechanisms how, when, and where NCP BVDV transfer across the placenta to infect the fetus occurs and how the persistently-infected fetus develops *in vivo*.

The eGFP2A gene with a 7 amino acid linker added to its N-terminus was selectively inserted between the N^{pro} gene and the nucleocapsid protein (C) gene of the viral genome. By this strategy, both authentic BVDV N^{pro} protein and the C-terminus of the eGFP2A protein were expected to be released from the viral precursor polyprotein as the autocatalytic activity of N^{pro} protein can cleave at its C-terminus between a proline-serine dipeptide motif (Rumenapf, *et al.*, 1998). The catalytic activity of FMDV 2A^{pro}

(Ryan, *et al.*, 1991, 1994; Percy, *et al.*, 1994) was expected to act on the proline-serine dipeptide motif at its C-terminus to release viral capsid protein with an additional N-terminal proline residue as well as releasing the eGFP2A protein. The reason we chose this region as the insertion site is that the genotype and phenotype of the recombinant virus was not likely to be impaired by the eGFP2A insert (Schweizer, *et al.*, 2001; Horscroft, *et al.*, 2005) which is critical for a recombinant BVDV virus that is to be used in animal testing *in vivo*.

It appears that the secondary structure of the viral RNA genome of BVDV is critical for viral replication and viral protein expression (Deng & Brock, 1992). In this study, we found that an eGFP2A insert was unstable when inserted into the viral genome and both point mutations and large deletions were detected in the N^{pro}/eGFP2A junction. Thus, the eGFP2A gene inserted into the viral genome appeared to provide a negative selection with strong influence on its genetic stability during viral replication. It is well known that viral RNA-dependent RNA polymerase is prone to inducing mutations in the viral genome. These were expected to occur in the eGFP2A insertion in BVDV genome during viral RNA replication. Surprisingly in this study, it was shown that two adjacent point mutations of A1626G and A1627G, which resulted in an amino acid substitution of lysine to glycine in the C-terminus of eGFP2A, conferred stability on the recombinant viral genome without other deletions or mutations presented in the N^{pro}/eGFP2A junction, the eGFP2A/C junction, or within the eGFP2A gene even after 10 passages of the virus in MDBK cells. Thus, a hypothesis is proposed that the eGFP2A insert impaired the stable secondary structure of the recombinant viral genome; however, the two adaptive

mutations in the eGFP2A insert stabilized the recombinant viral genome which was able to again form a stable secondary structure.

To investigate the impact of the eGFP2A insert on viral replication, we compared viral RNA replication and viral protein expression of the recombinant virus to that of wt SD1. We found that the stable eGFP2A insert had no detectable effect on the replication of the recombinant virus because both of the viruses showed similar levels of RNA replication (for both positive RNA replication and negative RNA replication) and viral protein expression. However, one-step growth analysis demonstrated that, although the replication kinetics of the recombinant virus and wt SD1 were similar and both viruses approach a maximum viral yield at approximately 60 hr post-infection, a peak yield of progeny virus of the recombinant virus was found to be approximately 0.5 log₁₀ lower than that of wt SD1 and the maximum yield of the recombinant virus was approximately 4 hr later than that of wt SD1. These results indicate that the eGFP2A insert may have slight impact on virion synthesis/assembly in the case of the recombinant virus. However, another explanation also exists such that, perhaps, the C protein in the recombinant virus, which has an additional proline residue added to its N-terminus, has an impact on virion synthesis/assembly for the recombinant virus or both.

BIBLIOGRAPHY

- Afshar, A, Dulac, G.C. and Howard, T. H. 1991. Comparative evaluation of the fluorescent antibody test and microtiter immunoperoxidase assay for detection of bovine viral diarrhea virus from bull semen. *Can. J. Vet. Res.* 55: 91-93.
- Alansari, H., Brock, K.V. and Potgieter, L.N.D. 1993. Single and double polymerase chain reaction for detection of bovine viral diarrhea virus in tissue culture and sera. *J. Vet. Diag. Invest.* 5: 148-153.
- Ames, T.R. and Baker, J.C. 1990. Management practices and vaccination programs that help control BVD virus infection. *Vet. Med.* 85: 1140-1149.
- Atluru, D., Xue, W., Polam, S., Atluru, S., Blecha, F. and Minocha, H.C. 1990. In vitro interactions of cytokines and bovine viral diarrhea virus in phytohemagglutinin stimulated bovine mononuclear cells. *Vet. Immunol. Immunopath.* 25:47-59.
- Baker, J. C. 1995. The clinical manifestations of bovine viral diarrhea infection. *Vet. Clin. North. Am.*, 11:425-445.
- Baker, J.C. 1987. Bovine viral diarrhea virus: A review. *J. Am. Vet. Med. Assoc.* 190:1449- 1457.
- Baker, J.C. 1990. Clinical aspects of bovine viral diarrhea virus infection. *Rev. Sci. Tech. Off. Int. Epiz.* 9:25-41.
- Becher, P., M. Orlich, A. Kosmidou, M. König, M. Baroth, and H.-J. Thiel. 1999. Genetic diversity of pestivirus: identification of novel groups and implications for classification. *Virology* 262:64–71.
- Bezek, D.M. and Mechor, G.D. 1992. Identification and eradication of bovine viral diarrhea virus in a persistently infected dairy herd. *J. Am. Vet. Med. Assoc.* 201:580-586.
- Bolin, S.R. 1993. Immunogens of bovine viral diarrhea virus. *Vet. Microbiol.* 37:263-271.
- Bolin, S.R. and Ridpath, J.F. 1989. Specificity of neutralizing and precipitating antibodies induced in healthy calves by monovalent modified-live bovine viral diarrhea virus vaccines. *Am. J. Vet. Res.* 50:817-821.

- Bolin, S.R. and Ridpath, J.F. 1990. Range of viral neutralizing activity and molecular specificity of antibodies induced in cattle by inactivated bovine viral diarrhea virus vaccines, *Am. J. Vet. Res.* 51:703-707.
- Bolin, S.R. and Ridpath, J.F. 1992. Differences in virulence between two noncytopathic bovine viral diarrhea viruses in calves. *Am. J. Vet. Res.* 53:2157-2163.
- Bolin, S.R., Littledike, E.T. and Ridpath, J.F. 1991. Serologic detection and practical consequences of antigenic diversity among bovine viral diarrhea viruses in a vaccinated herd. *Am. J. Vet. Res.* 52:1033-1037.
- Bolin, S.R., Moennig, V., Kelso, N.E. and Ridpath, J.F. 1988. Monoclonal antibodies with neutralizing activity segregate isolates of bovine viral diarrhea virus into groups. *Arch. Virol.* 99:117-123.
- Boye, M., Kamstrup, S. and Dalsgaard, K. 1991. Specific sequence amplification of bovine virus diarrhea virus (BVDV) and hog cholera virus and sequencing of BVDV nucleic acid. *Vet. Microbiol.* 29:1-13.
- Branza-Nichita, N., Durantel, D., Carrouee, S., Dwek, R.A., and Zitzmann, N. 2001. Antiviral effect of N-butyldeoxynojirimycin against bovine viral diarrhea virus correlated with misfolding of E2 envelope proteins and impairment of their association into E1-E2 heterodimers. *J. Virol.* 75:3527-3536.
- Brock, K.V. 1991. Detection of bovine viral diarrhea virus infections by DNA hybridization and polymerase chain reaction assay. *Arch. Virol. Suppl.* 3:199-208.
- Brock, K.V., Deng, R., Riblet, S.M. 1992. Nucleotide sequencing of 5' and 3' termini of bovine viral diarrhea virus by RNA ligation and PCR. *J. Virol. Meth.* 38:39-46.
- Brown, G.B., Zhang, H., Ping, L.-H. and Lemon, S.M. 1992. Secondary structure of the 5' nontranslated regions of hepatitis C virus and pestivirus genomic RNAs. *Nucleic Acids Res.* 20:5041-5045.
- Brownlie, J., Clarke, M.C. and Howard, C.J. 1987. Clinical and experimental mucosal disease-defining a hypothesis for pathogenesis. In *Pestivirus infections of ruminants*, ed. J. W. Harkness, pp.147-157.
- Brownlie, J. 1990. The pathogenesis of bovine viral diarrhea virus infection. *Rev. Sci. Tech. Off. Int. Epiz.* 9:43-59.
- Brownlie, J., Clarke, M.C., Hooper, L.B. and Bell, G.D. 1995 Protection of the bovine fetus from bovine viral diarrhea virus by means of a new inactivated vaccine. *Vet. Rec.* 137:58-62.

- Brownlie, J., Clarke, M.C. and Howard, C.J. 1989. Experimental infection of cattle in early pregnancy with a cytopathic strain of bovine virus diarrhoea virus. *Res. Vet. Sci.* 46:307-311.
- Carman, S., Van Dreume, T., Tremblay, R. et al. 1994. Severe acute bovine virus diarrhoea (BVD) in Ontario in 1993. In *Proceeding of the 37th Annual Meeting of the American Association of Veterinary Laboratory Diagnosticians*, Grand Rapids, MI, p. 19.
- Castrucci, G., Avellini, G., Cilli, V., Pedini, B., McKercher, D.O. and Valente, C. 1975. A study of immunologic relationships among serologically heterologous strains of bovine viral diarrhoea virus by cross immunity tests. *Cornell Vet.* 65:65-72.
- Cay, B., Chappuis, G., Coulibaly, C., Dintzer, Z. Edwards, S., Greiser-Wilke, I., Gunn, M., Have, P., Hess, G., Juntti, N., Liess, B., Mateo, A, McHugh, P., Moennig, V., Nettleton, P. and Wensvoort, O. 1989. Comparative analysis of monoclonal antibodies against pestiviruses: Report of an international workshop. *Vet. Microbiol.* 20:123-129.
- Collett, M. S., Wiskerchen, M.A., Welniak, E. and Belzer, S.K. 1991. Bovine viral diarrhoea virus genomic organization. *Arch. Virol. Suppl.* 3:19-27.
- Collett, M.S. 1992. Molecular genetics of pestiviruses. *Comp. Immun. Microbiol. Infect. Dis.* 15:145-154.
- Collett, M.S., Larson, R., Gold, C., Strick, B., Anderson, D.K. and Purchio, A.F. 1988. Molecular cloning and nucleotide sequence of the pestivirus bovine viral diarrhoea virus. *Virology* 165:191-199.
- Corapi, W.V., Donis, R.O. and Dubovi, E.J. 1988. Monoclonal antibody analyses of cytopathic and noncytopathic viruses from fatal bovine viral diarrhoea virus infections. *J. Virol.* 62:2823-2827.
- Corapi, W.V., Elliot, R.D., French, T.W., Arthur, D.G., Bezek, D.M. and Dubovi, E.J. 1990. Thrombocytopenia and hemorrhages in veal calves infected with bovine viral diarrhoea virus. *J. Am. Vet. Med. Assoc.* 196:590-596.
- Corapi, W.V., French, T.W. and Dubovi, E.J. 1989. Severe thrombocytopenia in young calves experimentally infected with noncytopathic bovine viral diarrhoea virus. *J. Virol.* 63:3934-3943.
- Coria, M.F. and McClurkin, A.W. 1978. Specific immune tolerance in an apparently healthy bull persistently infected with BVD virus. *J. Am. Vet. Med. Assoc.* 172:449-451.
- Cortese, V.S. 1994. No cause for alarm: Current BVD vaccines appear to cross-protect against virulent type 2 strains. *Topics. Vet. Med.* 5:10-14.

David, G.P., Crawshaw, T.R., Gunning, R.F., Hibberd, R.C., Lloyd, G.M. and Marsh, P.R. 1994. Severe disease in adult dairy cattle in three UK dairy herds associated with BVD virus infection. *Vet. Rec.* 134:468-472.

Davis, N. L., L. V. Willis, J. F. Smith, and R. E. Johnston. 1989. In vitro synthesis of infectious Venezuelan equine encephalitis virus RNA from a cDNA clone: analysis of a viable deletion mutant. *Virology* 171:189–204.

De Moerlooze, L., Lecomte, C., Brown-Shimmer, S., Schinetz, D., Guiot, C., Vandenberg, D., Allaer, D., Rossius, M., Chappuis, G., Dma, P., Renard, A. and Martial, J.A. 1993. Nucleotide sequence of the bovine viral diarrhea virus Osloss strain, comparison with related viruses and identification of specific DNA probes in the 5' untranslated region. *J. Gen. Virol.* 74:1433-1438.

Deng, R., and K. Brock. 1992. Molecular cloning and nucleotide sequence of a pestivirus genome, noncytopathogenic bovine viral diarrhea virus strain SD-1. *Virology* 191:867–879.

Deregt, D., Bolin, S.R., Heckert, R.A. and Loewen, K.G. 1994. Monoclonal antibodies to bovine viral diarrhea virus: cross-reactivities to field isolates and hog cholera virus strains. *Can. J. Vet. Res.* 58:71-74.

Desport, M., Collins, M.E. and Brownlie, J. 1994. Detection of bovine virus diarrhea virus RNA by in situ hybridization with digoxigenin-labelled riboprobes. *Intervirology* 37:269-276.

Donis, R.O. 1995. Molecular biology of bovine viral diarrhea virus and its interactions with the host. *Vet. Clinics North Am. – Food Animal Practice* 11:393-423.

Donis, R.O. and Dubovi, E.S. 1987. Molecular specificity of the antibody responses of cattle naturally and experimentally infected with cytopathic and noncytopathic of bovine biotypes of bovine virus diarrhea-mucosal disease virus. *Virology* 158:168-173.

Donis, R.O., Corapi, W.V. and Dubovi, E.S. 1988. Neutralizing monoclonal antibodies to BVDV bind to the 56K to 58K glycoprotein. *J. Gen. Virol.* 69:77-86.

Dubovi, E.J. 1992. Genetic diversity and BVD virus. *Comp. Immunol. Microbiol. Infect. Dis.* 15: 155-122.

Dubovi, E.J. 1990. The diagnosis of bovine viral diarrhea infections- a laboratory view. *Vet. Med.* 85:1133-1139.

Elbers, K., N. Tautz, P. Becher, D. Stoll, T. Rumenapf, and H.-J. Thiel. 1996. Processing in the pestivirus E2-NS2 region: identification of proteins p7 and E2p7. *J. Virol.* 70:4131–4135.

- Fenton, A., Entrican, G., Herring, J.A. and Nettleton, P.F. 1990. An ELISA for detecting pestivirus antigen in the blood of sheep persistently infected with border disease virus. *J. Virol. Meth.* 27:253-260.
- Fredriksen, B., Sandvik, T., Loken, T., Odegaard, S.A. 1999. Level and duration of serum antibodies in cattle infected experimentally and naturally with bovine viral diarrhoea virus. *Vet. Rec.* 114:111-114.
- Gottschalk, E.E., Greiser-Wilke I., Frey, H.R., Liess, B. and Moennig, V. 1992. An antigen capture test for detection of cattle viremic with bovine viral diarrhoea virus -a comparison with BVD virus isolations from bufi3' coat cells in bovine kidney cells. *J. Vet. Med. B.* 39:467-472.
- Grassmann, C.W., Isken, O., and Behrens, S.E. 1999. Assignment of the multifunctional NS3 protein of bovine viral diarrhoea virus during RNA replication: an in vivo and in vitro study. *Virology* 73:9196-9205.
- Greiser-Wilke, I., Haas, L., Dittmar, K. E., Liess, B. and Moennig, V. 1993. RNA insertions and gene duplications in the nonstructural protein p125 region of pestivirus strains and isolates in vitro and in vivo. *Virology* 193:977-980.
- Gruber, A., Greiser-Wilke, I., Haas, L., Hewicker-Trautwein, M. and Moennig, V. 1993. Detection of bovine viral diarrhoea virus RNA in formalin-fixed, paraffin-embedded brain tissue by nested polymerase chain reaction. *J. Virol. Meth.* 43:309-320.
- Gu, B., Liu, C., Lin-Goerke, D.R., Maley, L., Gutshall, L., Feltenberger, C.A., and Del Vecchio, A.N. 2000. The RNA helicase and nucleotide triphosphatase activities of the bovine viral diarrhoea virus NS3 protein are essential for viral replication. *J. Virol.* 74:1794-1800.
- Haines, T.M., Clark, E.G. and Dubovi, E.J. 1992. Monoclonal antibody-based immunohistochemical detection of bovine viral diarrhoea virus in formalin-fixed, paraffin-embedded tissues. *Vet. Pathol.* 29:27-32.
- Hamers, C., Dehan, P., Couvreur, B., Letellier, C., Kerkhofs, P., Pastoret, P.P., 2001. Diversity among bovine pestiviruses. *Vet. J.* 161:112-122.
- Harada, T., Tautz, N., and Thiel, H.J. 2000. E2-p7 region of the bovine viral diarrhoea virus polyprotein: processing and functional studies. *J. Virol.* 74:9498-9506.
- Harkness, J.W., Poeder, P.L, Drew, T., Wood, L. and Jeffrey, M. 1987. The efficacy of an experimental inactivated MVD-Mi) vaccine. In *Pestivirus infections of ruminants*.ed. 3rd. W. Harkness, pp.233-251.
- Hibberd, R.C., Turkington, A and Brownlie, J. 1993. Fatal bovine viral diarrhoea virus infection of adult cattle. *Vet. Rec.* 132:227-228.

- Hjerpe, C. A. 1990. Bovine vaccines and herd vaccination programs; Bovine viral diarrhoea (BVD) virus vaccines. *Vet. Clinics. North Am. – Food Animal Practice* 6:194-202.
- Hoofvanlddekinge, B.L., van Wamel, J.B., van Gennip, H.P, and Moormann, R.M. 1992. Application of the polymerase chain reaction to the detection of bovine viral diarrhoea virus infections in cattle. *Vet. Microbiol.* 30:21-34.
- Horscroft, N., Bellows, D., Ansari, I., Lai, V.C.H., Dempsey, S., Liang, D., Donis, R., Zhong, W. and Hong, Z. 2005. Establishment of a subgenomic replicon for bovine viral diarrhoea virus in Huh-7 cells and modulation of interferon-regulated factor 3-mediated antiviral response. *J. Virol.* 79:2788-2796.
- Howard, J.C. 1990. Immunological responses to bovine viral diarrhoea virus infections. *Rev. Sci. Tech. Off. Int. Epiz.* 9:95-103.
- Howard, J.C., Brownlie, J., and Clarke, M.C. 1987. Comparison by the neutralization assay of pairs of noncytopathogenic and cytopathogenic strains of bovine viral diarrhoea virus isolated from cases of mucosal disease. *Vet. Microbiol.* 13: 361-369.
- Howard, J.C., Clarke, M.C., Sopp, P., and Brownlie, J. 1992. Immunity to bovine viral diarrhoea virus in calves: the role of different T-cell subpopulations analysed by specific depletion in vivo with monoclonal antibodies. *Vet. Immunol. Immunopathol.* 32:303-314.
- Hulst, M.M., Himes, G., Newbiggin, E., and Moormann, R.J.M. 1994. Glycoprotein E2 of classical swine fever virus: expression in insect cells and identification as a ribonuclease. *Virology* 200:558–565.
- Hulst, M.M., Westra D.F., Wensvoort, G. and Moormann, R.J.M. 1993. Glycoprotein E1 of hog cholera virus expressed in insect cells protects swine from hog cholera. *J. Virol.* 67:5435-5442.
- Jensen, J., Aiken, J. and Schultz, R.D. 1990. Detection of bovine viral diarrhoea virus genome in leukocytes from persistently infected cattle by RNA-cDNA hybridization. *Can. J. Vet. Res.* 54:256-259.
- Kamstrap, S., Roensholt, L., and Dalsgaard, K. 1991. Immunological reactivity of bovine viral diarrhoea virus proteins after proteolytic treatment. *Arch. Virol. Suppl.* 3:225-230.
- Kao C.C., DelVecchio, A.M., and Zhong, W. 1999. De novo initiation of RNA synthesis by a recombinant flaviviridae RNA-dependent RNA polymerase. *Virology* 253:1-7.
- Katz, J.B., Ridpath, J.F. and Bolin, S.R. 1993. Presumptive diagnostic differentiation of hog cholera virus from bovine viral diarrhoea and border disease viruses by using a cDNA nested- amplification approach. *J. Clin. Microbiol.* 31:565-568.

- Kimman, T.G., Bianchi, A.T., Wensvoort, G., de Bruin, T.G., and Meliefste, C. 1993. Cellular immune response to hog cholera virus (HCV): T cells of immune pigs proliferate in vitro upon stimulation with live HCV, but the E1 envelope glycoprotein is not a major T-cell antigen. *J. Virol.* 67:2922-2927.
- Kirkland, P.D., McGowan, M.R. and Mackintosh, S.G. 1993. Factors influencing the development of persistent infection of cattle with pestivirus. In *Proceedings of the 2nd symposium on pestiviruses*, ed. S. Edwards, pp.117-121.
- König, M., Lengsfeld, T., Pauly, T., Stark, R., and Thiel, H.J. 1995. Classical swine fever virus: independent induction of protective immunity by two structural glycoproteins. *J. Virol.* 69:6479-6486.
- Kümmerer, B. M. and Meyers, G. 2000. Correlation between point mutations in NS2 and the viability and cytopathogenicity of bovine viral diarrhea virus strain Oregon analyzed with an infectious cDNA clone. *J. Virol.* 74:390-400.
- Kümmerer, B. M., Stoll, D., & Meyers, G. 1998. Bovine viral diarrhea strain Oregon: a novel mechanism for processing of NS2-3 based on point mutations. *J. Virol.* 72:4127-4138.
- Kupfermann, H., Thiel, H.J., Dubovi, E. J. & Meyers, G. 1996. Bovine viral diarrhea virus: characterization of a cytopathogenic defective interfering particle with two internal deletions. *J. Virol.* 70:8175-8181.
- Langedijk, J. P. 2002. Translocation activity of C-terminal domain of pestivirus E^{ns} and ribotoxin L3 loop. *J. Biol. Chem.* 277:5308-5314.
- Lazar, C., Zitzman, N., Dwek, R.A., and Branza-Nichita. 2003. The pestivirus Erns glycoprotein interacts with E2 in both infected cells and mature virions. *Virology.* 314:696-705.
- Liess, B., Orban, S., Frey, H.R., Trautwein, G., Weifel, W., and Blindow, H. 1984. Studies on transplacental transmissibility of a bovine viral diarrhea (BVD) vaccine virus in cattle. II Inoculation of pregnant cows without detectable neutralizing antibodies to BVD virus 90-220 days before perturbation (51st to 190th day of gestation). *Zentralbl. Veterinarmed. Reihe B.* 31:669-681.
- Lohmann, V., Overton, H., and Bartenschlager, R. 1999. Selective stimulation of hepatitis C virus and pestivirus NS5B RNA-dependent RNA polymerase activity by GTP. *J. Biol. Chem.* 274:10807-10815.
- Lopez, O.J., Osorio, F.A., Kelling, C.L., and Donis, R.O. 1993. Presence of bovine viral diarrhea virus in lymphoid cell populations of persistently infected cattle. *J. Gen. Virol.* 74:925-929.

- McClurkin, A. W., Coria, M.F., and Bolin, S.R. 1985. Isolation of cytopathic and noncytopathic bovine viral diarrhoea virus from the spleen of cattle acutely and chronically affected with bovine viral diarrhoea. *J. Am. Vet. Med. Assoc.* 186:568–569.
- McClurkin, A.W., Littledike, E.T., Cutlip, B.C., Frank, G.H., Coria, M.F. and Bolin, S.R. 1984. Production of cattle immunotolerant to bovine viral diarrhoea virus. *Can. J. Comp. Med.* 48:156-161.
- Mendez, E., Ruggli, N., Collett, M.S., and Rice, C.M. 1998. Infectious bovine viral diarrhoea virus (strain NADL) RNA from stable cDNA clones: a cellular insert determines NS3 production and viral cytopathogenicity. *J. Virol.* 72:4737-4745.
- Meyers, G. and Tauhiel, H. G. 1996. Molecular characterization of pestiviruses. *Adv. Virus. Res.* 47: 53-118.
- Meyers, G., Tauhiel, H. G. & Rumenapf, T. 1996. Classical swine fever virus: recovery of infectious viruses from cDNA constructs and generation of recombinant cytopathogenic defective interfering particles. *J. Virol.* 70: 1588-1595.
- Meyers, G., Tautz, N., Dubovi, E.J. and Thiel, H.J. 1991. Viral cytopathogenicity correlated with integration of ubiquitin-coding sequences. *Virology* 180:602-616.
- Meyers, G., Tautz, N., Stark, R., Brownlie, J., Dubovi, E.J., Collett, M.S., and Thiel, H.J. 1992. Rearrangement of viral sequences in cytopathogenic pestiviruses. *Virology* 191:368-386.
- Meyling A., Ronsholt, L., Dalsgaard, K., and Jensen, A.M. 1987. Experimental exposure of vaccinated and non-vaccinated pregnant cattle to isolates of bovine viral diarrhoea virus (BVDV). In *Pestivirus infections of ruminants*, ed. J. W. Harkness, pp.225-232.
- Moennig V. and Liess B. 1995. Pathogenesis of intrauterine infections with bovine viral diarrhoea virus. *Vet. Clin. North America.* 11:477-487.
- Moennig, V. (1990). Pestiviruses: a review. *Vet. Microbiol.* 23:35-54.
- Moennig, V., Frey, H.K., Liebler, E., Polenz, P. and Liess, B. 1990. Reproduction of muscosal disease with cytopathogenic bovine viral diarrhoea virus selected in vitro. *Vet. Rec.* 127:200-203.
- Nettleton, P.F. 1990. Pestivirus infections in ruminants other than cattle. *Rev. Sci. Tech. Off. Int. Epiz.* 9:131-150.
- Paton, D.J., Lowings, J.P., and Barrett, A.D. 1992. Epitope mapping of gp53 envelope protein of bovine viral diarrhoea virus. *Virology* 190:763-772.

Pellerin C., Van den Hurk J., Lecomte J., and Tijssen P. 1994. Identification of a new group of bovine viral diarrhoea virus strains associated with severe outbreaks and high mortalities. *Virology*. 203:260-8.

Percy, N., Barclay, W.S., García-Sastre, A., and Palese, P. 1994. Expression of a foreign protein by influenza A virus. *J. Virol.* 68: 4486–4492.

Perler, L., Schweizer, M., Jungi, T.W., and Peterhans, E. 2000. Bovine viral diarrhoea virus and bovine herpesvirus-1 prime uninfected macrophages for lipopolysaccharide-triggered apoptosis by interferon-dependent and independent pathways. *J. Gen. Virol.* 81:881-887.

Pestova, T. V., and Hellen, C.U. 1999. Internal initiation of translation in bovine viral diarrhoea virus. *Virology*. 258:249–256.

Pocock, D.H., Howard, C.J., Clarke, M.C., and Brownlie, J. 1987. Variation in the intracellular polypeptide profiles from different isolates of bovine viral diarrhoea virus. *Arch. Virol.* 94:43-53.

Poole, T.L., Wang, C., Popp, R.A., Potgieter, L.N.D., Siddiqui, A. and Collett, M.S. 1995. Pestivirus translation initiation occurs by internal ribosome entry. *Virology* 206:750-754.

Qi, F., Ridpath, J. F. and Berry, E. S. 1998. Insertion of a bovine SMT3B gene in NS4B and duplication of NS3 in a bovine viral diarrhoea virus genome correlate with the cytopathogenicity of the virus. *Virus Res.* 57:1–9.

Qi, F., Ridpath, J. F., Lewis, T., Bolin, S. R. and Berry, E. S. 1992. Analysis of the bovine viral diarrhoea virus genome for possible cellular insertions. *Virology* 189:285–292.

Radostitis, O.M. and Littlejohns, I.R. 1988. New concepts in the pathogenesis, diagnosis and control of disease caused by the bovine viral diarrhoea virus. *Can. Vet. J.* 29:513-528.

Renard, A, Guiot, C., Schnietz, D., Dagenais, L., Pastoret, P.P, Dina, D. and Martial, I.A. 1985. Molecular cloning of bovine viral diarrhoea virus sequences. *DNA* 4:429-438.

Rice, C. M. 1996. Flaviviridae: the viruses and their replication, p. 931–959. In B. N. Fields, D. M. Knipe, and P. M. Howley (ed.), *Fields virology*, 3rd ed. Lippincott-Raven, Philadelphia, Pa.

Rice, C. M., Levis, R., Strauss, J.H. and Huang, H.V. 1987. Production of infectious RNA transcripts from Sindbis virus cDNA clones: mapping of lethal mutations, rescue of a temperature-sensitive marker, and in vitro mutagenesis to generate defined mutants. *J. Virol.* 61:3809–3819.

Ridpath, I.F., Bolin, S.R. and Dubovi, E.J. 1994. Segregation of bovine viral diarrhoea virus into genotypes. *Virology* 205:66-74.

- Ridpath, J. F., and Bolin, S.R. 1995. The genomic sequence of a virulent bovine viral diarrhea virus (BVDV) from the type 2 genotype: detection of a large genomic insertion in a noncytopathic BVDV. *Virology* 212:39–46.
- Ridpath, J.F. and Bolin, S.R. 1991. Hybridization analysis of genomic variability among isolates of bovine viral diarrhea virus using cDNA probes. *Mol. Cell. Probes* 5:291-298.
- Ridpath, J.F., Bolin, S.R. and Katz, J. 1993. Comparison of nucleic acid hybridization and nucleic acid amplification using conserved sequences from the 5' noncoding region for the detection of bovine viral diarrhea virus. *J. Clin. Microbiol.* 31:986-989.
- Ridpath, J.F., Lewis, T.L., Bolin, S.R. and Berry, E.S. 1991. Antigenic and genomic comparison between non-cytopathic and cytopathic bovine viral diarrhea viruses isolated from cattle that had spontaneous mucosal disease. *J. Gen. Virol.* 72:725-729.
- Roberts, D.H., Lucus, M.H., Wibberley, G. and Westcott, D. 1988. Response of cattle persistently infected with bovine virus diarrhoea virus to bovine leukosis virus. *Vet. Rec.* 122:293-296.
- Rumenapf T., Stark, R. and Heimann M. 1998. N-terminal protease of pestiviruses: identification of putative catalytic residues by site-directed mutagenesis. *J. Virol.* 72:2544-2557.
- Rumenapf, T., Unger, G., Strauss, J.H. and Thiel, H.J. 1993. Processing of the envelope glycoproteins of pestiviruses. *J. Virol.* 67:3288-3294.
- Ryan, M. D., King, A.M.Q. and Thomas, G.D. 1991. Cleavage of foot-and-mouth disease virus polyprotein is mediated by residues located within a 19 amino acid sequence. *J. Gen. Virol.* 72:2727–2732.
- Ryan, M. D., and Drew, J. 1994. Foot-and-mouth disease virus 2A oligopeptide mediated cleavage of an artificial protein. *EMBO J.* 13:928–933.
- Sambrook, S., Fritsch, E.F. and Maniatis, T. 1989. *Molecular cloning: a laboratory manual*, 2nd ed. Cold Spring Harbor Laboratory Press, Cold Spring Harbor, N.Y.
- Schneider R., Unger, G., Stark, R., Schneider-Scherzer, E. and Thiel, H.J. 1993. Identification of a structural glycoprotein of an RNA virus as a ribonuclease. *Science* 261:1169–1171.
- Schweizer, M. and Perterhans, E. 2001. Noncytopathic bovine viral diarrhea virus inhibits double-stranded RNA-induced apoptosis and interferon aynthesis. *J. Virol.* 75:4692-4698.

- Schweizer, M. and Peterhans, E. 1999. Oxidative stress in cells infected with bovine viral diarrhea virus: a crucial step in the induction of apoptosis. *J. Gen. Virol.* 80:1147-1155.
- Shannon, A.D., Richards, S.G., Kirkland, P.D. and Moyle, A. 1991. An antigen-capture ELISA detects pestivirus antigens in blood and tissues of immunotolerant carrier cattle. *J. Virol. Meth.* 34:1-12.
- Stark R., Meyers, G., Rumenapf, T. and Thiel, H.J. 1993. Processing of pestivirus polyprotein: cleavage site between autoprotease and nucleocapsid protein of classical swine fever virus. *J. Virol.* 67:7088–7095.
- Sullivan, D.G., Chang, G.J., Trent, D.W. and Alkna, R.K. 1994. Nucleotide sequence analysis of the structural gene coding region of the pestivirus border disease virus. *Virus Res.* 33:219-228.
- Tautz, N., Meyers, G., Stark, R., Dubovi, E.J. and Thiel, H.J. 1996. Cytopathogenicity of a pestivirus correlates with a 27-nucleotide insertion. *J. Virol.* 70:7851-7858.
- Tautz, N., Elbers, K., Stoll, D., Meyers, G. and Thiel, H.J. 1997. Serine protease of pestiviruses: determination of cleavage sites. *J. Virol.* 71:5415–5422.
- Tautz, N., Thiel, H.J., Dubovi, E.J. and Meyer, G. 1994. Pathogenesis of mucosal disease: a cytopathogenic pestivirus generated by an internal deletion. *J. Virol.* 68: 3289-3297.
- Taylor, D.O.N., Gustafson, D.P. and Clafin, R.M. 1963. Properties of some viruses of the mucosal disease-virus diarrhea complex. *Am. J. Vet. Res.* 24:143-149.
- Taylor, L.F., Van Donkersgoed, J., Radostits, O.M., Booker, C.W., Dubovi, E.J., Van Den Hurk, J.V. and Janzen, E.D. 1994. Investigation of an outbreak of mucosal disease in a beef cattle herd in southwestern Saskatchewan. *Can. Vet. J.* 35:425-432.
- Thiel, H.J., Plagemann, G.W. and Moennig, V. 1996. The pestiviruses, p.1059–1073. In B. N. Fields, D. M. Knipe, and P. M. Howley (ed.), *Fields virology*, 3rd ed. Lippincott-Raven, Philadelphia, Pa.
- Thiel, H.J., Stark, R., Weiland, E., Rumenapf, T. and Meyer, G. 1991. Hog cholera virus: molecular composition of virions from a pestivirus. *J. Virol.* 65:4705-4712.
- Underdahl, N.R., Grace, O.D. and Hoerlein, A.B. 1957. Cultivation in tissue culture of cytopathogenic agent from bovine mucosal disease. *Proc. Soc. Exp. Biol. Med.* 94:795-797.
- Ward, P. and Misra, V. 1991. Detection of bovine viral diarrhea virus, using degenerate oligonucleotide primers and the polymerase chain reaction. *Am. J. Vet. Res.* 52:1231-1236.

- Weiland, E., Stark, R., Haas, B., Rumenapf, T., Meyers, G. and Thiel, H.J. 1990. Pestivirus glycoprotein which induces neutralizing antibodies forms part of a disulfide-linked heterodimer. *J. Virol.* 64:3563–3569.
- Wensvoort, G. 1989. Topographical and functional mapping of epitopes on hog cholera virus with monoclonal antibodies. *J. Gen. Virol.* 70:2865-2876.
- Windisch, J. M., Schneider, R., Stark, R., Weiland, E., Meyers, G. and Thiel, H.J 1996. RNase of classical swine fever virus: biochemical characterization and inhibition by virus-neutralizing monoclonal antibodies. *J. Virol.* 70:352–358.
- Wiskerchen, M. Belzer, S.K. and Collett, M.S. 1991. Pestivirus gene expression: the first protein product of the bovine viral diarrhea virus large open reading frame, p20, possesses proteolytic activity. *J. Virol.* 65:4508-4514.
- Xu, J., Mendez, E., Caron, P.R., Lin, C., Murcko, M.A., Collett, M.S. and Rice, C.M. 1997. Bovine viral diarrhea virus NS3 serine proteinase: polyprotein cleavage sites, cofactor requirements, and molecular model of an enzyme essential for pestivirus replication. *J. Virol.* 71:5312–5322.
- Xue, W. and Minocha, H.C. 1993. Identification of the cell surface receptor for bovine viral diarrhea virus by using anti-idiotypic antibodies. *J. Gen. Virol.* 74:73-79.
- Xue, W., Blecha, F. and Minocha, H.C. 1990. Antigenic variations in bovine viral diarrhea viruses detected by monoclonal antibodies. *J. Clin. Microbiol.* 28:688-693.
- Zhong, W., Gutshall, L.L. and Del Vecchio, A.M. 1998. Identification and characterization of an RNA-dependent RNA polymerase activity within the nonstructural protein 5B region of bovine viral diarrhea virus. *J. Virol.* 72:9365-9369.

APPENDIX

Plasmid

1. pUCMCS

Nucleotide primers PUCPOSF and PUCNEGF were annealed to generate a cloning adaptor. This adaptor was subcloned into the *NarI-HindIII* sites of pUC19 resulting in pUCMCS with the introduced restriction sites by the adaptor.

2. pUCEH

Nucleotide primers PUCEHP and PUCEHN were annealed to generate a cloning adaptor. This adaptor was subcloned into the *EcoRI-HindI* sites of pUC19 to resulting in pUCEH with the introduced sites by the adaptor.

3. pUCNDE

The Nucleotide primers PUCMCSP and PUCMCSN were annealed to generate a cloning adaptor. This adaptor was subcloned into the *NarI-PacI* sites of pUC19.

4. pUCNDEH

Nucleotide primers PUCMCSP and PUCMCSN were annealed to generate a cloning adaptor. This adaptor was subcloned into the *NarI-PacI* sites of pUC19.

5. pBADEH

Nucleotide primers PUCEHP and PUCEHN were annealed to generate a cloning adaptor. This adaptor was subcloned into the *EcoRI-HindIII* sites of pBAD24. The introduced restriction sites in pBADEH includes

6. peGFP2A1

The six-nucleotide deletion of AAGAAC in peGFP2A was repaired by site-directed mutagenesis using peGFP2A as template and eGFP-AAGAAC-P and eGFP-AAGAAC-N as nucleotide primers. This plasmid contains the original eGFP2A sequence.

7. pSDXN

A 1.9kb *XbaI-NdeI* fragment was obtained from the RT-PCR product amplified from the wt SD1 genome using nucleotide primer pair SD1-*XbaI*-T7 and BVD2094N and

subcloned into the *XbaI-NdeI* sites of the pUCMCS vector. This plasmid contains the SD1 sequence between nucleotides 1 and 1924 with a point mutation of A1472G.

8. pSDXN1

A1472G in pSDXN was repaired by site-directed mutagenesis using pSDXN as template and SD1-1472P and SD1-1472N as nucleotide primers. This plasmid contains the SD1 sequence between nucleotides 1 and 1924.

9. pSDNF

A 2.3 kb *NdeI-FseI* fragment was obtained from the RT-PCR product amplified from the wt SD1 genome using nucleotide primer pair BVD1793 and 4636L18 and subcloned into the *NdeI-FseI* sites of the pUCMCS vector. This plasmid contains the SD1 sequence between nucleotides 1925 and 4204.

10. pSDFN

A 1.8 kb *FseI-NsiI* fragment was obtained from the RT-PCR product amplified from the wt SD1 genome using nucleotide primer pair 4190U18 and BVD6374 and subcloned into the *FseI-NsiI* sites of the pUCNDEH vector. This plasmid contains the SD1 sequence between nucleotides 4205 and 6000 with a four-nucleotide deletion of ACTT between nucleotide 4455 and 4458.

10. pSDFN1

The four-nucleotide deletion of ACTT between nucleotide 4455 and 4458 of the wt SD1 genome was repaired by site-directed mutagenesis using pSDFN as template and SD1-4455-4458ACTT-P and SD1-4455-4458ACTT-N as nucleotide primers. This plasmid contains the SD1 sequence between nucleotides 4205-6000.

11. pSDNE

A 900 bp *NsiI-EagI* fragment was obtained from the RT-PCR product amplified from the wt SD1 genome using nucleotide primer pair BVD5830 and BVD6951 and subcloned into the *NsiI-EagI* sites of the pUCMCS vector. This plasmid contains the SD1 sequence between nucleotides 6001 and 6900 with two point mutations of G6278A and A6858T.

12. pSDNE1

G6278A in pSDNE was repaired by site-directed mutagenesis using pSDNE as template and SD1-6278P and SD1-6278N as nucleotide primers. This plasmid contains the SD1 sequence between nucleotides 6001 and 6900 with a point mutation of A6858T.

13. pSDNE2

A6858T in pSDNE1 was repaired by site-directed mutagenesis using pSDNE1 as template and SD1-6858P and SD1-6858N as nucleotide primers. This plasmid contains the SD1 sequence between nucleotides 6000 and 6900.

14. pSDEN

A 1.6 kb *EagI-NcoI* fragment was obtained from the RT-PCR product amplified from the wt SD1 genome using nucleotide primer pair SD16891 and BVD8523 and subcloned into the *EagI-NcoI* sites of the pUCNDEH vector. This plasmid contains the SD1 sequence between nucleotides 6901 and 8461 with two silent mutations of T7585C and G7882C.

15. pSDNN

A 1.7 kb *NcoI-NdeI* fragment was obtained from the RT-PCR product amplified from the wt SD1 genome using nucleotide primer pair BVD8313 and BVD10545 and subcloned into the *NcoI-NdeI* sites of the pUCNDEH vector. This plasmid contains the SD1 sequence between nucleotides 8462 and 10126 with one point mutation of T8748G and one silent mutation of G9022A.

16. pSDNN1

T8748G in pSDNN was repaired by site-directed mutagenesis using pSDNN as template and SD1-8748P and SD1-8748N as nucleotide primers. This plasmid contains the SD1 sequence between nucleotides 8462 and 10126 with a silent mutation of G9022A.

17. pSDNP

A 2.2 kb *NdeI-PacI* fragment was obtained from the RT-PCR product amplified from the wt SD1 genome using nucleotide primer pair BVD9985 and SD1-SdaI-PacI and subcloned into the *NdeI-PacI* sites of the pUCMCS vector. This plasmid contains the SD1 sequence between nucleotides 10127 and 12319 with two point mutations of G10583C and A12264G, one silent mutation of A10912G and a one-nucleotide deletion of A at nt 12089.

18. pSDNP1

G10583C in pSDNP was repaired by site-directed mutagenesis using pSDNP as template and SD1-10583P and SD1-10583N as nucleotide primers. This plasmid contains the SD1 sequence between nucleotides 10127 and 12319 with two point mutations of A10912G and A12264G and a one-nucleotide deletion of A at nt 12089.

19. pSDNP2

A one-nucleotide deletion of A at nt 12089 in pSDNP1 was repaired by site-directed mutagenesis using pSDNP1 as template and SD1-12089P and SD1-12089N as nucleotide primers. This plasmid contains the SD1 sequence between nucleotides 10127 and 12319 with a silent mutation of A10912G and a point mutation of A12264G.

20. pUCSDFE

A 1.8 kb *FseI-NsiI* fragment was isolated from pSDFN1 and a 900 bp *NsiI-EagI* fragment was isolated from pSDNE1. These two DNA fragments were subcloned into the *FseI-EagI* sites of the pSDEN vector by three-way ligation. This plasmid contains the SD1 sequence between nucleotides 4205 and 6901 with two point mutations of G10583C and A12264G, one silent mutation of A10912G and a one-nucleotide deletion of A at nt 12089.

21. pUCSDEN

A 1.6 kb *EagI-NcoI* fragment was isolated from pSDEN and a 1.7 kb *NcoI-NdeI* fragment was isolated from pSDNN1. These two DNA fragments were subcloned into the *EagI-NdeI* sites of the pUCNDEH vector by three-way ligation. This plasmid contains the SD1 sequence between nucleotides 6000 and 10126 with two point mutations of G10583C and A12264G, one silent mutation of A10912G and a one-nucleotide deletion of A at nt 12089.

22. pACXF

A 1.9 kb *XbaI-NdeI* fragment was isolated from pSDXN1 and a 2.3 kb *NdeI-PacI* fragment was isolated from pSDNF. These two DNA fragments were subcloned into the *XbaI-PacI* sites of the pACSD1 vector. This plasmid contains the SD1 sequence between nucleotides 1 and 4204.

23. pSDFB

A 750 bp *FseI-BamHI* fragment was obtained from the PCR product amplified from pSDFN using nucleotide primers SD1-UP-FseI and SD1-DOWN-BamHI and subcloned back to the *FseI-BamHI* site of pSDFN. This plasmid contains the SD1 sequence between nucleotides 4205 and 4981 with a silent mutation of C4981A.

24. pSDFN1-INS

A 1.0 kb *ApaI-NsiI* fragment was obtained from the PCR product amplified from pSDFN using nucleotide primers SD1-UP-ApaI and SD1-DOWN-NsiI and a 50 bp *BamHI-ApaI* fragment was obtained by annealing two nucleotide primers PSDFNP and PSDFNN. These two fragments were subcloned into the *BamHI-NsiI* sites of pSDFB by three way ligation. This plasmid contains the SD1 sequence of 4205 and 6000 with a 48 bp insertion at nt 4982. Also this plasmid contains two silent mutations of C4981A and A4990G.

25. pBADFP-INS

A 1.8 kb *FseI-NsiI* fragment was isolated from pSDFN1-INS and subcloned into the *FseI-NsiI* sites of pBADFP. This plasmid contains the SD1 sequence of 4205 to 12318 with a 48 bp insertion together with two silent mutations of C4981A and A4990G.

26. pUCB

A 7.5 kb *HindIII* fragment was isolated from pBeloBACII and subcloned into the *HindIII*-CIP site of the pUC19 vector. This plasmid contains the whole nucleotide sequence of pBeloBACII.

27. pUCEHF

A 2.7 kb *BsrGI-HindIII* fragment was isolated from pBeloBACII and subclone into the *BsrGI-HindIII* sites of the pUCEH vector.

28. pUCEHFXBAI

The *XbaI* site in pUCEHF was removed by site-directed mutagenesis using nucleotide primers PBELOXBAP and PBELOXBAN.

29. pUCBXBAI

A 2.7 kb *BsrGI-HindI* fragment was isolated from pUCEHFXBAI and subcloned into the *BsrGI-HindI* sites of pUCB.

30. pBAS

Nucleotide primers PUCPOSF and PUCNEGF were annealed to generate a cloning adaptor. A 7.0 kb *NarI-SfiI* fragment was isolated from pUCBXBAI. The adaptor was ligated to the 7.0 kb *NarI-SfiI* fragment resulting in a vector with the SP6 and T7 promoters were removed from the pBeloBACII backbone.

31. pUCBAS

A 7.0 kb *HindIII* fragment was isolated from pBAS and subcloned into the *HindIII*-CIP site of pUC19.

32. pSDFN1- Δ XBAI

The *XbaI* site in pSDFN1 was removed by site-directed mutagenesis using nucleotide primers SD1-5308-*XbaI*-P and SD1-5308-*XbaI*-N. This plasmid has the same nucleotide sequence as pSDFN1 with an exception of a point mutation of A5308G which inactivated the *XbaI* restriction site.

33. pUCSDFE- Δ XBAI

A 1.1 kb *FseI-SalI* fragment was isolated from pSDFN1- Δ XBAI and subcloned into the *FseI-SalI* sites of the pUCSDFE vector. This plasmid has the same SD1 sequence except the A5308G nucleotide substitution which inactivated the *XbaI* site.

34. pBADFP- Δ XBAI

A 2.7 kb *FseI-EagI* fragment was isolated from pUCSDFE- Δ XBAI and subcloned into the *FseI-EagI* sites of the pBADFP vector. This plasmid contains the SD1 sequence between nucleotides 4205 and 12319 with five silent mutations of A5308G, T7585C, G7882C, G9022A and A10912G and one point mutation of A12264G.

35. pBSD1- Δ XBAI

A 4.2 kb *XbaI-FseI* fragment was isolated from pACXF, an 8.1 kb *FseI-PacI* fragment was isolated from pBADFP- Δ XbaI, and a 7.0 kb *XbaI-PacI* fragment was isolated from pUCBAS. These three fragments were ligated together by three-way ligation. This plasmid contains the whole SD1 sequence with five silent mutations of A5308G, T7585C, G7882C, G9022A and A10912G and one point mutation of A12264G in a pBeloBACII backbone.

36. pBSD1

A 4.2 kb *XbaI-FseI* fragment was isolated from pACXF, an 8.1 kb *FseI-PacI* fragment was isolated from pBADFP, and a 7.0 kb *XbaI-PacI* fragment was isolated from pUCBAS. These three fragments were ligated together by three-way ligation. This plasmid contains the whole SD1 sequence with four silent mutations of T7585C, G7882C, G9022A and A10912G and one point mutation of A12264G in a pBeloBACII backbone.

37. pBSD1-ΔXBAl

A 4.2 kb *XbaI-FseI* fragment was isolated from pACXF, an 8.1 kb *FseI-PacI* fragment was isolated from pBADFP-ΔXBAl, and a 7.0 kb *XbaI-PacI* fragment was isolated from pUCBAS. These three fragments were ligated together by three-way ligation. This plasmid contains the whole SD1 sequence with five silent mutations of A5308G, T7585C, G7882C, G9022A and A10912G and one point mutation of A12264G in a pbeloBACII backbone.

38. pBADFP

A 2.7 kb *FseI-EagI* fragment was isolated from pUCSDFE, a 3.3 kb *EagI-NdeI* fragment was isolated from pUCSDEN, and a 2.3 kb *NdeI-PacI* fragment was isolated from pSDNP2. These three fragments were subcloned into the *FseI-PacI* sites of pBADEH by four-way ligation. This plasmid contains the SD1 sequence between nucleotides 4205 and 12319 with four silent mutations of T7585C, G7882C, G9022A and A10912G and one point mutation of A12264G.

39. pSDNF3895

Site-directed mutagenesis was performed using nucleotide primers of SD1-3895-P and SD1-3895-N and pSDNF as template. This plasmid contains the SD1 sequence between nucleotides 1925 and 4204 with a silent mutation of A3895G which created a *KpnI* restriction site.

40. pFAN15

A 768 bp *KpnI* fragment was obtained from the PCR product amplified from peGFP2A1 using nucleotide primer pair eGFP-UP-*KpnI* and eGFP-DOWN-*KpnI* and subcloned into the *KpnI*-CIP site of pSDNF3895.

41. pACXF-eGFP2A1-3895

A 3.0 kb *NdeI-FseI* fragment was isolated from pFAN15 and subcloned into the *NdeI-FseI* sites of pACXF. This plasmid contains the SD1 sequence between nucleotides of 1 and 4204 with a 768 bp eGFP2A insert at nt 3895.

42. pSDNF3817

Site-directed mutagenesis was performed using nucleotide primers of SD1-3819-3822-TACC-N and SD1-3819-3822-TACC-P and pSDNF as template. This plasmid contains the SD1 sequence between nucleotides 1925 and 4204 with nucleotides substitution of GTCA to TACC at nt 3819 to 3822 which created a *KpnI* restriction site.

43. FAN14

A 768 bp *KpnI* fragment was obtained from the PCR product amplified from peGFP2A1 using nucleotide primer pair eGFP-UP-*KpnI* and eGFP-DOWN-*KpnI* and subcloned into the *KpnI*-CIP site of pSDNF3817.

44. pACXF-eGFP2A1-3817

A 3.0 kb *NdeI-FseI* fragment was isolated from pFAN14 and subcloned into the *NdeI-FseI* sites of pACXF. This plasmid contains the SD1 sequence between nucleotides of 1 and 4204 with a 768 bp eGFP2A insertion at nt 3817.

45. pSDNF-eGFP2A

A 768 bp *SfiI* fragment was obtained from the PCR product amplified from pEGFP2A using nucleotide primer pair eGFP-UP-SfiI and eGFP-DOWN-SfiI and subcloned into the *SfiI* site of pSDNF. This plasmid contains the SD1 sequence between nucleotides of 1925 and 4204 with a 768 bp eGFP2A insert at nt 3581.

46. pFAN20

Site-directed mutagenesis was performed using nucleotide primers of eGFP-AAGAAC-P and eGFP-AAGAAC-N and pSDNF-eGFP2A as template. This plasmid contains the SD1 sequence between nucleotides 1925 and 4204 with the original eGFP2A1 insertion at nt 3581.

47. pACXF-eGFP

A 3.0 kb *NdeI-FseI* fragment was isolated from pSDNF-eGFP2A and subcloned into the *NdeI-FseI* sites of pACXF. This plasmid contains the SD1 sequence between nucleotides of 1 and 4204 with a 768 bp eGFP2A insert at nt 3581.

48. pcDNA-SD1-C890

A 300 bp *KpnI-NotI* fragment was obtained from the PCR product amplified from pASD1 using nucleotide primer pair SD1-890-KpnI and SD1-1195-NotI and subcloned into the *KpnI-NotI* sites of the pcDNA3.1 Zeo (+) vector. This plasmid contains the SD1 sequence between nucleotides 890 and 1195.

49. pcDNA-SD1-C893

A 300 bp *KpnI-NotI* fragment was obtained from the PCR product amplified from pASD1 using nucleotide primer pair SD1-893-KpnI and SD1-1195-NotI and subcloned into the *KpnI-NotI* sites of the pcDNA3.1 Zeo (+) vector. This plasmid contains the SD1 sequence between nucleotides 893 and 1195

50. pcDNA-SD1-N^{pro}-C

An 800 bp *KpnI-NotI* fragment was obtained from the PCR product amplified from pASD1 using nucleotide primer pair SD1-386-KpnI and SD1-1195-NotI and subcloned into the *KpnI-NotI* sites of the pcDNA3.1 Zeo (+) vector. This plasmid contains the SD1 sequence between nucleotides 386 and 1195

51. pcDNA-INS-NADL-C890

A 300 bp *KpnI-NotI* fragment was obtained from the PCR product amplified from pASD1 using nucleotide primer pair INS-NADL-890-KpnI and INS-NADL-1195-NotI and subcloned into the *KpnI-NotI* sites of the pcDNA3.1 Zeo (+) vector. This plasmid contains the XINS-NADL sequence between nucleotides 890 and 1195

52. pcDNA-INS-NADL-C893

A 300 bp *KpnI-NotI* fragment was obtained from the PCR product amplified from pASD1 using nucleotide primer pair INS-NADL-893-*KpnI* and SD1-1195-*NotI* and subcloned into the *KpnI-NotI* sites of the pcDNA3.1 Zeo (+) vector. This plasmid contains the SD1 sequence between nucleotides 893 and 1195.

53. pcDNA-INS-NADL-N^{pro}-C

An 800 bp *KpnI-NotI* fragment was obtained from the PCR product amplified from pASD1 using nucleotide primer pair INS-NADL-386-*KpnI* and INS-NADL-1195-*NotI* and subcloned into the *KpnI-NotI* sites of the pcDNA3.1 Zeo (+) vector. This plasmid contains the SD1 sequence between nucleotides 386 and 1195.

54. pFAN1

A 1.0 kb *XbaI-ApaI* fragment was obtained from the PCR product amplified from pXINS-NADL using nucleotide primers SD1-T7-*XbaI* and XINS-NADL-955-*ApaI* and a 800 bp *ApaI-NdeI* fragment was obtained from the PCR product amplified from pASD1 using nucleotide primers SD1-1118-*ApaI* and SD1-1924-*NdeI*. These two fragments were subcloned into the *XbaI-NdeI* sites of pUCMCS by three-way ligation.

55. pFAN2

A 450 bp *XbaI-ApaI* fragment was obtained from the PCR amplification from pASD1 using nucleotide primers SD1-T7-*XbaI* and SD1-442-*ApaI* and an 800 bp *ApaI-NdeI* fragment was obtained from the PCR product amplified from pASD1 using nucleotide primers SD1-1118-*ApaI* and SD1-1924-*NdeI*. These two fragments were subcloned into the *XbaI-NdeI* sites of pUCMCS by three-way ligation.

56. pSDXN-ΔN^{pro}-C

A1472G in pFAN2 was repaired by site-directed mutagenesis using pFAN2 as template and SD1-1472P and SD1-1472N as nucleotide primers.

57. pFAN3

A 1.0 kb *XbaI-ApaI* fragment was obtained from the PCR product amplified from pASD1 using nucleotide primers SD1-T7-*XbaI* and SD1-955-*ApaI* and an 800 bp *ApaI-NdeI* fragment was obtained from the PCR product amplified from pASD1 using nucleotide primers SD1-1118-*ApaI* and SD1-1924-*NdeI*. These two fragments were subcloned into the *XbaI-NdeI* sites of pUCMCS by three-way ligation.

58. pFAN6

A1472G in pFAN3 was repaired by site-directed mutagenesis using pFAN3 as template and SD1-1472P and SD1-1472N as nucleotide primers.

59. pFAN7

An 800 bp *ApaI-NdeI* fragment was obtained from the PCR product amplified from pXINS-NADL using nucleotide primers SD1-1118-*ApaI* and XINS-NADL-1924-*NdeI* was subcloned into the *ApaI-NdeI* sites of the pFAN1 vector.

60. pSDXN-ΔC

A1472G in pFAN4 was repaired by site-directed mutagenesis using pFAN4 as template and SD1-1472P and SD1-1472N as nucleotide primers.

61. pACXF-ΔN^{pro}-C

A 1.3 kb *XbaI-NdeI* fragment was isolated from pSDXN1-ΔN^{pro}-C and a 2.3 kb *NdeI-PacI* fragment was isolated from pSDNF. These two fragments were subcloned into the *XbaI-PacI* sites of the pACSD1 vector.

62. pACXF-ΔC

A 1.7 kb *XbaI-NdeI* fragment was isolated from pSDXN1-ΔC and a 2.3 kb *NdeI-PacI* fragment was isolated from pSDNF. These two fragments were subcloned into the *XbaI-PacI* sites of the pACSD1 vector.

63. pASD1-ΔN^{pro}-C

An 8.2 kb *FseI-PacI* fragment was isolated from pBADFP and subcloned into the *FseI-PacI* sites of pACXF-ΔN^{pro}-C. This plasmid contains the whole SD1 sequence with a T7 promoter fused upstream of the 3'-UTR, a *SdaI* site attached downstream of the 5'-UTR, and four silent mutations of T7585C, G7882C, G9022A and A10912G and one point mutation of A12264G. Additionally, nt 368 to 1194 of the SD1 sequence were deleted in this plasmid.

64. pASD1-ΔC

An 8.2 kb *FseI-PacI* fragment was isolated from pBADFP and subcloned into the *FseI-PacI* sites of pACXF-ΔC. This plasmid contains the whole SD1 sequence with a T7 promoter fused upstream of 3'-UTR, a *SdaI* site attached downstream of 5'-UTR, and four silent mutations of T7585C, G7882C, G9022A and A10912G and one point mutation of A12264G. Additionally, nt 889 to 1194 of the SD1 sequence were deleted in this plasmid.

65. pFAN4

A 450 bp *XbaI-ApaI* fragment was obtained from the PCR product amplified from pXINS-NADL using nucleotide primers SD1-T7-*XbaI* and SD1-442-*ApaI* and an 800 bp *ApaI-NdeI* fragment was obtained from the PCR product amplified from pASD1 using nucleotide primers SD1-1118-*ApaI* and SD1-1924-*NdeI*. These two fragments were subcloned into the *XbaI-NdeI* sites of pUCMCS by three-way ligation.

66. pXINS-NADL-XN-ΔN^{pro}-C

A1472G in pFAN4 was repaired by site-directed mutagenesis using pFAN4 as template and SD1-1472P and SD1-1472N as nucleotide primers.

67. pFAN5

A1472G in pFAN1 was repaired by site-directed mutagenesis using pFAN1 as template and SD1-1472P and SD1-1472N as nucleotide primers. This plasmid contains the SD1 sequence between nucleotides 1 and 1924 with a deletion of nt 443 to 1120.

68. pXINS-NADL-XN-ΔC

A1472G in pFAN1 was repaired by site-directed mutagenesis using pFAN1 as template and SD1-1472P and SD1-1472N as nucleotide primers.

69. pFAN16

Site-directed mutagenesis was performed using nucleotide primers eGFP-AAGAAC-P and eGFP-AAGAAC-N and pFAN10 as template. This plasmid contains the SD1 sequence between nucleotides 1 and 1924 with the original eGFP2A insert.

70. pFAN17

Site-directed mutagenesis was performed using nucleotide primers eGFP-AAGAAC-P and eGFP-AAGAAC-N and pFAN11 as template. This plasmid contains the SD1 sequence between nucleotides 1 and 1924 with the original eGFP2A insert.

71. pFAN18

Site-directed mutagenesis was performed using nucleotide primers eGFP-AAGAAC-P and eGFP-AAGAAC-N and pFAN12 as template. This plasmid contains the SD1 sequence between nucleotides 1 to 1924 with the original eGFP2A insertion.

72. pFAN19

Site-directed mutagenesis was performed using nucleotide primers eGFP-AAGAAC-P and eGFP-AAGAAC-N and pFAN13 as template. This plasmid contains the SD1 sequence between nucleotides 1 and 1924 with the original eGFP2A insert.

73. pACXF-eGFP2A1-16

A 2.7 kb *XbaI-NdeI* fragment was isolated from pFAN16 and subcloned into the *XbaI-NdeI* sites of pACXF. This plasmid contains the SD1 sequence between nucleotides of 1 and 4204 with a 768 bp eGFP2A1 insert.

74. pACXF-eGFP2A1-17

A 2.7 kb *XbaI-NdeI* fragment was isolated from pFAN17 and subcloned into the *XbaI-NdeI* sites of pACXF. This plasmid contains the SD1 sequence between nucleotides of 1 and 4204 with a 768 bp eGFP2A1 insert.

75. pACXF-eGFP2A1-18

A 2.7 kb *XbaI-NdeI* fragment was isolated from pFAN18 and subcloned into the *XbaI-NdeI* sites of pACXF. This plasmid contains the SD1 sequence between nucleotides of 1 and 4204 with a 768 bp eGFP2A1 insert.

76. pACXF-eGFP2A1-19

A 2.7 kb *XbaI-NdeI* fragment was isolated from pFAN19 and subcloned into the *XbaI-NdeI* sites of pACXF. This plasmid contains the SD1 sequence between nucleotides of 1 and 4204 with a 768 bp eGFP2A1 insert.

77. pFAN8

A 1.0 kb *ApaI-NdeI* fragment was obtained from the PCR product amplified from pSDXN1 using nucleotide primers SD1-890-*ApaI* and SD1-1924-*NdeI* and subcloned into the *ApaI-NdeI* sites of the pFAN2 vector.

78. pFAN9

A 1.0 kb *ApaII-NdeI* fragment was obtained from the PCR product amplified from pSDXN1 using nucleotide primers SD1-893-*ApaI* and SD1-1924-*NdeI* and subcloned into the *ApaI-NdeI* sites of the pFAN2 vector.

79. pACXF-eGFP2A3

A 1.0 kb *SacI-AatII* fragment was obtained from the RT-PCR product amplified from ASD1-eGFP2A1 genome using nucleotide primers BVD424 and BVD1172 and subcloned into the *SacI-AatII* sites of the pACXF. This plasmid contains the SD1 sequence between nucleotides of 1 and 4204 with a 768 bp eGFP2A1 insert which harbors two point mutations of A715G and A716G in eGFP2A1 sequence.

80. pFAN10

A 900 bp *XbaI-KpnI* fragment was obtained from the PCR product amplified from pSDXN1 using nucleotide primer pair SD1-T7-*XbaI* and SD1-917-*KpnI* and a 760 bp *KpnI-ApaI* fragment was obtained from the PCR product amplified from peGFP2A using nucleotide primer pair eGFP-UP-*KpnI* and eGFP-DOWN-*KpnI*. These two fragments were subcloned into the *XbaI-ApaI* sites of pFAN8 by three-way ligation.

81. pFAN11

A 900 bp *XbaI-KpnI* fragment was obtained from the PCR product amplified from pSDXN1 using nucleotide primer pair SD1-T7-*XbaI* and SD1-917-*KpnI* and a 760 bp *KpnI-ApaI* fragment was obtained from the PCR product amplified from peGFP2A using nucleotide primer pair eGFP-UP-*KpnI* and eGFP-DOWN-*KpnI*. These two fragments were subcloned into the *XbaI-ApaI* sites of pFAN9 by three-way ligation.

82. pFAN12

A 760 bp *ApaI* fragment was obtained from the PCR product amplified from peGFP2A using nucleotide primer pair eGFP-UP-*ApaI* and eGFP-DOWN-*KpnI* and subcloned into the *ApaI-CIP* site of pFAN8.

83. pFAN13

A 760 bp *ApaI* fragment was obtained from the PCR product amplified from peGFP2A using nucleotide primer pair eGFP-UP-*ApaI* and eGFP-DOWN-*KpnI* and subcloned into the *ApaI-CIP* site of pFAN9.

84. pACXF-eGFP2A-M

A 2.7 kb *XbaI-NdeI* fragment was isolated from pFAN10 and subcloned into the *XbaI-NdeI* sites of pACXF. This plasmid contains the SD1 sequence between nt 1 and 4204 with 768 bp eGFP2A insert which have a six-nucleotide deletion of AAGAAC from nt 715 to 720 in the eGFP2A insert.

85. pACXF-eGFP2A-N

A 2.7 kb *XbaI-NdeI* fragment was isolated from pFAN11 and subcloned into the *XbaI-NdeI* sites of pACXF. This plasmid contains the SD1 sequence between nt 1 and 4204 with 768 bp eGFP2A insert which have a six-nucleotide deletion of AAGAAC from nt 715 to 720 in the eGFP2A insert.

86. pACXF-eGFP2A-O

A 2.7 kb *XbaI-NdeI* fragment was isolated from pFAN12 and subcloned into the *XbaI-NdeI* sites of pACXF. This plasmid contains the SD1 sequence between nt 1 and 4204 with 768 bp eGFP2A insert which have a six-nucleotide deletion of AAGAAC from nt 715 to 720 in the eGFP2A insert.

87. pACXF-eGFP2A-P

A 2.7 kb *XbaI-NdeI* fragment was isolated from pFAN13 and subcloned into the *XbaI-NdeI* sites of pACXF. This plasmid contains the SD1 sequence between nt 1 and 4204 with 768 bp eGFP2A insert which have a six-nucleotide deletion of AAGAAC from 715 to 720 in the eGFP2A insert.

88. pASD1

An 8.2 kb *FseI-PacI* fragment was isolated from pBADFP and subcloned into the *FseI-PacI* sites of pACXF. This plasmid contains the whole SD1 sequence with a T7 promoter fused upstream of the 3'-UTR, a *SdaI* site attached downstream of the 5'-UTR, and four silent mutations of T7585C, G7882C, G9022A and A10912G and one point mutation of A12264G. (Unstable)

89. pASD1-eGFP2A1 (pASD1-eGFP2A1-16)

An 8.2 kb *FseI-PacI* fragment was isolated from pBADFP and subcloned into the *FseI-PacI* sites of pACXF-eGFP2A1-16. (Unstable)

90. pASD1-eGFP2A2 (pASD1-eGFP2A1-17)

An 8.2 kb *FseI-PacI* fragment was isolated from pBADFP and subcloned into the *FseI-PacI* sites of pACXF. (Unstable)

91. pASD1-eGFP2A3

An 8.2 kb *FseI-PacI* fragment was isolated from pBADFP and subcloned into the *FseI-PacI* sites of pACXF-eGFP2A3. (Unstable)

92. pASD1-N^{pro}/eGFP2A (pASD1-eGFP2A1-18)

An 8.2 kb *FseI-PacI* fragment was isolated from pBADFP and subcloned into the *FseI-PacI* sites of pACXF-eGFP2A1-18. (Unstable)

93. pASD1-N^{pro}/2AeGFP2A

An 8.2 kb *FseI-PacI* fragment was isolated from pBADFP and subcloned into the *FseI-PacI* sites of pACXF-eGFP2A1-20. (Unstable)

94. pASD1-IN

An 8.2 kb *FseI-PacI* fragment was isolated from pBADFP-IN and subcloned into the *FseI-PacI* sites of pACXF. (Unstable)

95. pBADPE

A 2.7 kb *FseI-EagI* fragment was isolated from pUCSDFE and subcloned into the *FseI-EagI* sites of the pBADPF vector. This plasmid contains the SD1 sequence between nt 4205 and 12319 with three coding mutations of T8748G, G10583C, and A12264G; four noncoding mutations of T7575C, G7882C, G9022A and A10912G; a one-nucleotide deletion of A at nt 12089.

96. pBADPF

An 8.1 kb *FseI-PacI* fragment was isolated from pACSD1 and subcloned into the *FseI-PacI* sites of the pBADEH vector. This plasmid contains the SD1 sequence between nt 4205 and 12319 with five coding mutations of G6278A, A6858T, T8748G, G10583C, and A12264G; four noncoding mutations of T7575C, G7882C, G9022A and A10912G; a one-nucleotide deletion of A at nt 12089; and a four-nucleotide deletion of ACTT between nt 4455 and 4458.

97. pBADPN

A 3.2 kb *EagI-NdeI* fragment was isolated from pUCSDEN and subcloned into the *EagI-NdeI* sites of the pBADPE vector. This plasmid contains the SD1 sequence between nt 4205 and 12319 with two coding mutations of G10583C and A12264G; four noncoding mutations of T7575C, G7882C, G9022A and A10912G; a one-nucleotide deletion of A at nt 12089.

98. pUCSDXN (pUCSDX)

A 3.5 kb *XmaI-NdeI* fragment was isolated from pACSD1 and subcloned into the *XmaI-NdeI* sites of the pUC19 vector. This plasmid contains the SD1 sequence between nt 6686 and 10126 with two coding mutations of A6858T and T8748G, three noncoding mutations of T7575C, G7882C and G9022A.

99. pUCSDXN1 (pUCSDXM)

The point mutation of T8748G in pUCSDXN was repaired using SD1-8748P and SD1-8748N as nucleotide primers and site-directed mutagenesis.

100. pACEN

A 7.0 kb *XbaI-PacI* fragment was isolated from pBADPN and subcloned into the *XbaI-PacI* sites of the pACSD1 vector. (Not stable)

101. pACXN

A 1.7 kb *XbaI-EagI* fragment was isolated from pUCSDFE and subcloned into the *XbaI-EagI* sites of the pACEN vector. (Not stable)

102. pACXE

A 4.2 kb *XbaI-FseI* fragment was isolated from pACXF and a 2.7 kb *FseI-PacI* fragment was isolated from pUCSDFE. These two fragments were subcloned into the *XbaI-PacI* sites of the pACSD1. (Not stable)

103. pACXP

A 2.3 kb *NdeI-PacI* fragment was isolated from pSDNP2 and subcloned into the *NdeI-PacI* sites of the pACXN vector. (Not stable)

RECOMBINANT VIRUSES

1. ASD1

pASD1 was linearized with *SdaI* and *in vitro* transcription was performed with T7 RNA polymerase. The transcript was electroporated into MDBK cells and rescued virus was designated as ASD1. RT-PCR and nucleotide sequencing indicated ASD1 contains all five genetic markers as designed.

2. ASD1-IN

pASD1-IN was linearized with *SdaI* and *in vitro* transcription was performed with T7 RNA polymerase. The transcript was electroporated into MDBK cells and rescued virus was designated as ASD1-IN. RT-PCR and nucleotide sequencing indicated ASD1 contains all the five genetic markers and the 16 amino acid insertion as designed.

3. ASD1-eGFP2A1

pASD1-eGFP2A1 was linearized with *SdaI* and *in vitro* transcription was performed with T7 RNA polymerase. The transcript was electroporated into MDBK cells and rescued virus was designated as ASD1-eGFP2A1. Deletion(s) and mutation(s) occurred in the N^{pro}/eGFP2A junction. (eGFP2A insertion was not stable in the viral genome).

4. ASD1-eGFP2A2

pASD1-eGFP2A2 was linearized with *SdaI* and *in vitro* transcription was performed with T7 RNA polymerase. The transcript was electroporated into MDBK cells and rescued virus was designated as ASD1-eGFP2A2. Deletions(s) and mutation(s) occurred in the N^{pro}/eGFP2A junction. (eGFP2A insertion was not stable in the 'viral genome).

5. ASD1-eGFP2A3

pASD1-eGFP2A3 was linearized with *SdaI* and *in vitro* transcription was performed with T7 RNA polymerase. The transcript was electroporated into MDBK cells and rescued virus was designated as ASD1-eGFP2A3. (eGFP2A insertion with two point mutations of A1662G and A1663G was stably maintained in the viral genome).

6. ASD1-N^{pro}/eGFP2A

pASD1-N^{pro}/eGFP2A was linearized with *SdaI* and *in vitro* transcription was performed with T7 RNA polymerase. The transcript was electroporated into MDBK cells and rescued virus was designated as ASD1-N^{pro}/eGFP2A. (eGFP2A stably expressed in MDBK cells).

7. ASD1-N^{pro}/2AeGFP2A

pASD1-N^{pro}/2AeGFP2A was linearized with *SdaI* and *in vitro* transcription was performed with T7 RNA polymerase. The transcript was electroporated into MDBK cells and rescued virus was designated as ASD1-N^{pro}/2AeGFP2A. (eGFP2A stably expressed in MDBK cells).

8. BSD1

pBSD1 was linearized with *SdaI* and *in vitro* transcription was performed with T7 RNA polymerase. The transcript was electroporated into MDBK cells and rescued virus was designated as BSD1.

9. XINS-NADL

pXINS-NADL was linearized with *SdaI* and *in vitro* transcription was performed with T7 RNA polymerase. The transcript was electroporated into MDBK cells and rescued virus was designated as XINS-NADL.

10. ASD1-eGFP2A-3895

pASD1-eGFP2A-3895 was linearized with *SdaI* and *in vitro* transcription was performed with T7 RNA polymerase. The transcript was electroporated into MDBK cells and rescued virus was designated as ASD1-eGFP2A-3895. (eGFP2A insertion in the viral genome was not checked).